

Polynomial iteration complexity of a path-following smoothing Newton method for symmetric cone programming

Yu-Hong Dai · Ruoyu Diao · Xin-Wei Liu ·
Rui-Jin Zhang

Abstract It has long remained open whether smoothing Newton methods (SNMs) for symmetric cone programming (SCP) admit polynomial iteration complexity. A key difficulty lies in the lack of an analogue of the self-concordant convex framework underlying interior-point methods (IPMs). In this paper, inspired by Nemirovski's self-concordant convex-concave theory, we address this open problem by introducing a reduced barrier augmented Lagrangian (BAL) function. We prove that the reduced BAL function is self-concordant convex-concave and establish that the parameterized smooth system arising in SNMs coincides with the first-order optimality conditions of an associated minimax problem. Motivated by this equivalence, we propose a path-following smoothing Newton method (PFSNM). The reduced BAL function induces a central path and an associated neighborhood, which provide estimates for the Newton decrement needed for the path-following analysis. As a result, the method achieves an iteration complexity of $\mathcal{O}(\sqrt{\nu} \ln(1/\varepsilon))$, matching the best-known short-step complexity for IPMs. Numerical results on standard benchmarks show that PFSNM is competitive with several well-known interior-point solvers, and the observed performance is consistent with the theoretical development.

Keywords Smoothing Newton method · Path-following method · Symmetric cone · Self-concordant convex-concave function · Polynomial iteration complexity

Mathematics Subject Classification (2020) 90C60 · 90C25 · 65K05

The authors are listed in alphabetical order.

Yu-Hong Dai · Ruoyu Diao

State Key Laboratory of Mathematical Sciences, Academy of Mathematics and Systems Science, Chinese Academy of Sciences, and the University of Chinese Academy of Sciences, Beijing, China

E-mail: dyh@lsec.cc.ac.cn, diaoruoyu18@mails.ucas.ac.cn

Xin-Wei Liu

Institute of Mathematics, Hebei University of Technology, Tianjin, China

E-mail: mathlxw@hebut.edu.cn

Rui-Jin Zhang (Corresponding author)

School of Mathematical Sciences and LPMC, Nankai University, Tianjin, China

E-mail: zhangrj@nankai.edu.cn

1 Introduction

Symmetric cone programming (SCP) is a fundamental class of convex optimization problems that includes linear programming (LP), second-order cone programming (SOCP), semidefinite programming (SDP), and their Cartesian products. Let \mathbb{E} be a Euclidean Jordan algebra equipped with a bilinear operation “ \circ ” and an identity element e , and let $\mathbb{K} \subseteq \mathbb{E}$ be the associated symmetric cone, i.e., a closed convex cone that is both self-dual and homogeneous. We consider the standard primal-dual form of SCP:

$$\begin{aligned} \text{(P)} \quad & \min \{ \langle c, x \rangle \mid \mathcal{A}x = b, x \in \mathbb{K} \}, \\ \text{(D)} \quad & \max \{ \langle b, \lambda \rangle \mid \mathcal{A}^* \lambda + s = c, s \in \mathbb{K} \}, \end{aligned} \tag{1}$$

where $c, x, s \in \mathbb{E}$ and $b, \lambda \in \mathbb{R}^m$. The linear operator $\mathcal{A} : \mathbb{E} \rightarrow \mathbb{R}^m$ is assumed to be surjective, and \mathcal{A}^* denotes its adjoint. We assume that the Slater condition holds for both (P) and (D), which is a standard assumption in SCP.

Interior-point methods (IPMs) are among the most important algorithms for symmetric cone programming. They replace the complementarity condition $x \circ s = 0$ in the Karush–Kuhn–Tucker (KKT) system of (1) by $x \circ s = \mu e$ with $\mu > 0$, which yields the perturbed KKT system

$$\mathcal{A}x = b, \mathcal{A}^* \lambda + s = c, x, s \in \text{int}(\mathbb{K}), x \circ s = \mu e. \tag{2}$$

The solutions of this system form the central path. IPMs trace this path as $\mu \downarrow 0$. Their complexity theory is based on a self-concordant convex framework [33], which induces a local metric, yields estimates for the Newton decrement, and provides a natural way to define neighborhoods of the central path. In SCP, this framework leads to the classical polynomial iteration complexities: an $\mathcal{O}(\sqrt{\nu} \ln(1/\varepsilon))$ iteration complexity for short-step methods [9, 10, 38, 43, 45] and an $\mathcal{O}(\nu \ln(1/\varepsilon))$ iteration complexity for long-step methods [9, 32, 35, 38, 45], where ν denotes the rank of \mathbb{K} and ε is the target accuracy. These worst-case complexities explain why IPMs admit a remarkably robust global theory while retaining strong practical performance.

Alongside IPMs, smoothing Newton methods (SNMs) constitute another important class of algorithms for SCP. The basic idea is to reformulate the KKT system as a system of nonsmooth equations and then smooth the complementarity condition. This yields the parameterized smooth system

$$\mathcal{A}x = b, \mathcal{A}^* \lambda + s = c, \Phi(x, s; \mu) = 0, \tag{3}$$

where Φ is a chosen smoothing function and μ is driven to zero via a continuation strategy [8, 19, 20, 36]. Common choices for Φ include the smoothing Fischer–Burmeister (FB) function [20, 37] and the smoothing Chen–Harker–Kanzow–Smale (CHKS) function [7, 20, 39]. Unlike IPMs, SNMs do not require the iterates to remain strictly in the interior and are therefore sometimes called non-interior continuation methods. The first non-interior path-following method was proposed by Chen and Harker [7]. Subsequently, Burke and Xu [5] established the first global linear convergence result for a non-interior path-following method for linear complementarity problems, and later proved its local quadratic convergence under suitable assumptions [4]. Qi, Sun, and Zhou [37] gave a new formulation of smoothing Newton methods for nonlinear complementarity problems and box-constrained

variational inequalities, thereby providing a unified framework that strongly influenced later developments of SNMs. For further advances and related results on SNMs, we refer the reader to [6, 19, 22, 23, 25, 41] and the references therein.

Despite these appealing convergence results, SNMs have lacked a polynomial iteration complexity guarantee, which has remained a long-standing open problem (see Burke and Xu [5] and Kanzow [20]). A key difficulty is that classical SNMs do not admit an analogue of the self-concordant convex framework that underlies the polynomial complexity theory of IPMs. Such a framework provides a central path, a neighborhood structure defined by an appropriate merit function, and the Newton-decrement estimates required for path-following analysis. These are fundamental because they give estimates for the descent of the merit function when μ is updated, which are typically hard to obtain without the framework.

Several attempts have been made to address this problem. One line of research incorporates the parameterized smooth system into an interior-point framework. A representative example is the interior-point path-following algorithm proposed by Xu and Burke [46], which uses the smoothing CHKS function to generate a rescaled Newton direction within the interior-point framework and achieves a polynomial complexity. However, its iterates are still required to stay in the interior of the cone. In contrast, Hotta, Inaba, and Yoshise [18] proposed an SNM based on the smoothing CHKS function that eliminates the interior-point requirement, but with a non-polynomial complexity of $\mathcal{O}(\varepsilon^{-6} \ln \varepsilon^{-2})$, which is far from the standard polynomial iteration complexities of IPMs. Hence, the following central problem is still open:

Can smoothing Newton methods for symmetric cone programming attain polynomial iteration complexity?

In this paper, we answer this question affirmatively. Our approach is inspired by the self-concordant convex-concave framework introduced by Nemirovski [31], which provides a natural viewpoint for extending self-concordant ideas from convex minimization to saddle-point problems. The key step is to introduce a reduced barrier augmented Lagrangian (BAL) function that reveals the minimax structure underlying SNMs. We show that this reduced BAL function is self-concordant convex-concave, and that the parameterized smooth system associated with SNMs coincides with the first-order optimality conditions of a minimax problem with the reduced BAL function as the objective. This equivalence induces a local metric for SNMs, enabling the definition of a central path and an associated neighborhood analogous to those in the interior-point framework. More importantly, it provides the Newton decrement estimates required to control the path-following process. On this basis, we propose a path-following smoothing Newton method (PFSNM) for SCP and establish a worst-case iteration complexity of $\mathcal{O}(\sqrt{\nu} \ln(1/\varepsilon))$, which matches the best-known short-step complexity for IPMs on symmetric cones. To the best of our knowledge, this is the first polynomial iteration complexity result for a smoothing Newton method in the general SCP setting.

Although our main focus is theoretical, the resulting method is also computationally attractive. PFSNM admits a Newton system with an explicit Schur-complement structure, leading to an efficient system-formation procedure. Furthermore, numerical experiments on standard benchmark problems show that PFSNM is competitive with several well-known interior-point solvers. These results are consistent with the established polynomial-complexity theory.

1.1 Organization

The remainder of the paper is organized as follows. Section 2 reviews preliminaries on Euclidean Jordan algebras and self-concordant convex-concave functions. Section 3 introduces the reduced BAL function, establishes its self-concordant convex-concave property, and characterizes the parameterized smooth system via an equivalent minimax formulation. Section 4 presents the proposed path-following smoothing Newton method and the associated merit functions. Section 5 analyzes the effect of updating the smoothing parameter on the merit functions and derives the polynomial iteration complexity of the proposed method. Numerical results are reported in Section 6 and illustrate the practical effectiveness of PFSNM. The paper concludes in Section 7. Auxiliary technical proofs are deferred to Appendix A.

1.2 Notation

Throughout the paper, $\hat{\mathbb{E}}$ and \mathbb{E} denote finite-dimensional Euclidean spaces. For an integer $k \geq 1$, let $C^k(\mathbb{E}, \hat{\mathbb{E}})$ denote the space of k -times continuously differentiable functions from \mathbb{E} to $\hat{\mathbb{E}}$; if $\hat{\mathbb{E}} = \mathbb{R}$, we write $C^k(\mathbb{E}) := C^k(\mathbb{E}, \mathbb{R})$. For $f \in C^k(\mathbb{E})$, let $D^k f(x)[h_1, \dots, h_k]$ denote the k -th differential of f at x along directions $h_1, \dots, h_k \in \mathbb{E}$. Then $D^k f(x)$ is a symmetric k -linear form. In particular, $D^2 f(x) : \mathbb{E} \rightarrow \mathbb{E}$ is also a linear operator, satisfying

$$\langle h_1, D^2 f(x)h_2 \rangle = D^2 f(x)[h_1, h_2], \quad \forall h_1, h_2 \in \mathbb{E}.$$

The gradient of f at x is denoted by $\nabla f(x)$ and is defined by

$$\langle \nabla f(x), h \rangle = Df(x)[h], \quad \forall h \in \mathbb{E}.$$

For $g \in C^k(\hat{\mathbb{E}} \times \mathbb{E})$ and $w = (\hat{x}, s) \in \hat{\mathbb{E}} \times \mathbb{E}$, we write $\nabla_{\hat{x}} g(w)$ and $\nabla_s g(w)$ for the partial gradients, $D_{\hat{x}} g(w)$ and $D_s g(w)$ for the corresponding partial derivatives. Let $\mathcal{W}, \mathcal{H} : \mathbb{E} \rightarrow \mathbb{E}$ be linear operators. We write $\mathcal{H} \succ \mathcal{W}$ if

$$\langle h, \mathcal{H}h \rangle > \langle h, \mathcal{W}h \rangle, \quad \forall h \in \mathbb{E} \setminus \{0\}.$$

In particular, $\mathcal{H} \succ 0$ means $\langle h, \mathcal{H}h \rangle > 0$ for all nonzero $h \in \mathbb{E}$. The interior of a cone \mathbb{K} is denoted by $\text{int}(\mathbb{K})$. Additional notation will be introduced as needed.

2 α -self-concordant convex-concave functions

This section reviews the core concepts needed in the subsequent analysis. We begin by introducing Euclidean Jordan algebras, which provide the algebraic foundation for symmetric cones and thus play a central role in symmetric cone optimization. We then revisit and generalize the theory of α -self-concordant convex-concave functions.

2.1 Euclidean Jordan algebras and symmetric cones

Definition 1 A Jordan algebra (\mathbb{E}, \circ) is a finite-dimensional vector space over the real field \mathbb{R} with a bilinear mapping $\circ : \mathbb{E} \times \mathbb{E} \rightarrow \mathbb{E}$ such that, for all $x, y, z \in \mathbb{E}$,

$$x \circ y = y \circ x, \quad x^2 \circ (x \circ y) = x \circ (x^2 \circ y), \quad \text{where } x^2 := x \circ x.$$

The algebra is called Euclidean if there exists an inner product, denoted by $\langle \cdot, \cdot \rangle$, which is associative, i.e., for all $x, y, z \in \mathbb{E}$,

$$\langle x \circ y, z \rangle = \langle x, y \circ z \rangle.$$

A crucial property of Euclidean Jordan algebras is that every element admits a spectral decomposition, which generalizes the eigenvalue decomposition of a symmetric matrix.

Theorem 1 *Let \mathbb{E} be a Euclidean Jordan algebra of rank ν . For any $z \in \mathbb{E}$, there exist pairwise orthogonal primitive idempotents $\{v_1, \dots, v_\nu\}$ and unique real eigenvalues $\lambda_1(z), \dots, \lambda_\nu(z)$ such that*

$$z = \sum_{i=1}^{\nu} \lambda_i(z) v_i, \quad (4)$$

where the idempotents satisfy

$$\sum_{i=1}^{\nu} v_i = e, \quad v_i \circ v_j = 0 \text{ for all } i \neq j, \quad \text{and } v_i \circ v_i = v_i \text{ for all } i.$$

By the spectral decomposition, the trace and determinant of z are defined analogously to those of a real matrix:

$$\text{tr}(z) := \sum_{i=1}^{\nu} \lambda_i(z), \quad \det(z) := \prod_{i=1}^{\nu} \lambda_i(z). \quad (5)$$

An element z lies in the interior of the cone \mathbb{K} if and only if all its eigenvalues are strictly positive; in particular, $\det(z) > 0$. The spectral decomposition also enables a functional calculus on \mathbb{E} . Given a scalar function $g : \mathbb{R} \rightarrow \mathbb{R}$ and an element $z \in \mathbb{E}$ with the spectral decomposition $z = \sum_{i=1}^{\nu} \lambda_i(z) v_i$, define

$$g(z) := \sum_{i=1}^{\nu} g(\lambda_i(z)) v_i. \quad (6)$$

This definition allows for operations such as the square root $z^{1/2}$, the inverse z^{-1} , and the logarithm $\ln(z)$.

By [14, Proposition III.1.5], the bilinear form $\text{tr}(x \circ y)$ is symmetric, positive definite, and associative. Thus, $\text{tr}(x \circ y)$ defines an inner product. In the sequel, we denote this inner product by $\langle x, y \rangle$, i.e.,

$$\langle x, y \rangle := \text{tr}(x \circ y). \quad (7)$$

In the following, we present three commonly used symmetric cones and their algebraic properties, which are essential to the development of our algorithm.

Table 1: Common types of symmetric cones.

Cone	Mathematical representation	Jordan product	Spectral decomposition
Nonnegative orthant	$\mathbb{R}_+^n = \{x \in \mathbb{R}^n \mid x_i \geq 0, \forall i = 1, \dots, n\}$	$x \circ y := \text{Diag}(x)y$	$x = \sum_{i=1}^n x_i e_i$
Second-order cone	$\mathbb{Q}^{n+1} = \{(x_0; \bar{x}) \in \mathbb{R} \times \mathbb{R}^n \mid x_0 \geq \ \bar{x}\ _2\}$	$x \circ y := \text{Arw}(x)y^a$	$x = \lambda_1 v_1 + \lambda_2 v_2^b$
Positive semidefinite cone	$\mathbb{S}_+^n = \{X \in \mathbb{R}^{n \times n} \mid X \succeq 0\}$	$X \circ Y := \frac{1}{2}(XY + YX)$	$X = \sum_{i=1}^n \lambda_i v_i v_i^{\top c}$

^a $\text{Arw}(x) := \begin{pmatrix} x_0 & \bar{x}^\top \\ \bar{x} & x_0 I_{n \times n} \end{pmatrix}$.

^b Let $\tilde{v} \in \mathbb{R}^n$ satisfy $\|\tilde{v}\| = 1$. Then the eigenvalues of x are $\lambda_1 = x_0 + \|\bar{x}\|$ and $\lambda_2 = x_0 - \|\bar{x}\|$, and the corresponding primitive idempotents are

$$v_1 = \begin{cases} \frac{1}{2} \begin{pmatrix} 1; \frac{\bar{x}}{\|\bar{x}\|} \end{pmatrix}, & \text{if } \bar{x} \neq 0; \\ \frac{1}{2} (1; \tilde{v}), & \text{if } \bar{x} = 0, \end{cases} \quad v_2 = \begin{cases} \frac{1}{2} \begin{pmatrix} 1; -\frac{\bar{x}}{\|\bar{x}\|} \end{pmatrix}, & \text{if } \bar{x} \neq 0; \\ \frac{1}{2} (1; -\tilde{v}), & \text{if } \bar{x} = 0. \end{cases}$$

^c $\{\lambda_i\}_{i=1}^n$ are the eigenvalues of X , and $\{v_i v_i^\top\}_{i=1}^n$ are the corresponding primitive idempotents.

2.2 α -self-concordant convex-concave functions

In this subsection, we review the definition and basic properties of α -self-concordant convex-concave functions. They provide the theoretical tools for analyzing Newton's method for finding saddle points. We begin with the classical notion of self-concordant convex functions.

Definition 2 ([31, Definition 2.1]) Let \mathbb{E} be a Euclidean Jordan algebra, $\mathbb{X} \subset \mathbb{E}$ be an open convex domain, and $\alpha > 0$. A convex function $f \in C^3(\mathbb{X})$ is called α -self-concordant on \mathbb{X} if the following conditions hold:

- (i) f is a barrier for \mathbb{X} , i.e., $f(x^{(k)}) \rightarrow \infty$ along every sequence of points $x^{(k)} \in \mathbb{X}$ converging to the boundary of \mathbb{X} .
- (ii) For all $x \in \mathbb{X}$ and $h_x \in \mathbb{E}$,

$$\left| D^3 f(x)[h_x, h_x, h_x] \right| \leq \frac{2}{\alpha^{1/2}} \left(D^2 f(x)[h_x, h_x] \right)^{3/2}. \quad (8)$$

If $\alpha = 1$, f is called standard self-concordant. An α -self-concordant convex function f is said to be nondegenerate if $D^2 f(x) \succ 0$ for all $x \in \mathbb{X}$.

It is well known that an α -self-concordant convex function satisfies a Dikin ellipsoid bound, which characterizes the local geometry induced by its second-order derivative.

Theorem 2 ([33, Theorem 2.1.1]) Let \mathbb{E} be a Euclidean Jordan algebra and $\mathbb{X} \subset \mathbb{E}$ be an open convex domain. Let f be an α -self-concordant convex function on \mathbb{X} , $x \in \mathbb{X}$, and $\Delta x \in \mathbb{E}$. If $r := \sqrt{\frac{1}{\alpha} D^2 f(x)[\Delta x, \Delta x]} < 1$, then $x + \Delta x \in \mathbb{X}$ and for all $h_x \in \mathbb{E}$,

$$(1-r)^2 D^2 f(x)[h_x, h_x] \leq D^2 f(x + \Delta x)[h_x, h_x] \leq \frac{1}{(1-r)^2} D^2 f(x)[h_x, h_x]. \quad (9)$$

Each symmetric cone \mathbb{K} admits a natural barrier function (see [44, Section 2.6]) $\phi : \text{int}(\mathbb{K}) \rightarrow \mathbb{R}$, defined as

$$\phi(x) := -\ln(\det(x)).$$

By [17], $\phi \in C^\infty(\text{int}(\mathbb{K}))$ is a nondegenerate standard self-concordant convex function on $\text{int}(\mathbb{K})$. For every $x \in \text{int}(\mathbb{K})$, the second-order derivative $D^2\phi(x) \succ 0$. Consequently, the inverse operator $(D^2\phi(x))^{-1} : \mathbb{E} \rightarrow \mathbb{E}$ is well defined and satisfies $(D^2\phi(x))^{-1} \succ 0$. In particular, the gradient and second-order derivative of ϕ satisfy

$$\nabla\phi(x) = -x^{-1}, \quad \langle \nabla\phi(x), (D^2\phi(x))^{-1}\nabla\phi(x) \rangle = \nu, \quad \forall x \in \text{int}(\mathbb{K}). \quad (10)$$

The subsequent analysis focuses on α -self-concordant convex-concave functions. We consider unconstrained minimax problems whose objective is convex in the minimization variables and concave in the maximization variables. To extend Newton's method to this setting, it is essential to identify a class of convex-concave functions that exhibits geometric properties similar to those of self-concordant convex functions. This motivates the concept of α -self-concordant convex-concave functions, which generalizes the definition in [31].

Definition 3 Let $\hat{\mathbb{E}}$ and \mathbb{E} be finite-dimensional Euclidean spaces, $f(\hat{x}, s) \in C^3(\hat{\mathbb{E}} \times \mathbb{E})$, and $\alpha > 0$. The function f is called α -self-concordant convex-concave on $\hat{\mathbb{E}} \times \mathbb{E}$ if the following conditions hold:

- (i) f is convex in $\hat{x} \in \hat{\mathbb{E}}$ for every $s \in \mathbb{E}$, and concave in $s \in \mathbb{E}$ for every $\hat{x} \in \hat{\mathbb{E}}$.
- (ii) For every $w = (\hat{x}, s) \in \hat{\mathbb{E}} \times \mathbb{E}$ and $h = (h_{\hat{x}}, h_s) \in \hat{\mathbb{E}} \times \mathbb{E}$,

$$\left| D^3 f(w)[h, h, h] \right| \leq \frac{2}{\alpha^{1/2}} (S_f(w)[h, h])^{3/2}, \quad (11)$$

where $S_f(w)[h, h] := D_{\hat{x}\hat{x}}^2 f(w)[h_{\hat{x}}, h_{\hat{x}}] - D_{ss}^2 f(w)[h_s, h_s]$.

If $\alpha = 1$, f is called standard self-concordant convex-concave. An α -self-concordant convex-concave function f is called nondegenerate if the quadratic form $S_f(w)$ is positive definite for all $w \in \hat{\mathbb{E}} \times \mathbb{E}$.

Remark 1 The concept of an α -self-concordant convex-concave function can also be defined on an open convex domain (see [31]). The only difference is that, in that setting, the functions $f(\cdot, s)$ and $-f(\hat{x}, \cdot)$ are required to be barriers, respectively. In contrast, our analysis is carried out on the entire space $\hat{\mathbb{E}} \times \mathbb{E}$, which has no boundary. Therefore, no barrier property is required in our definition.

The following proposition relates nondegenerate α -self-concordant convex-concave functions to nondegenerate α -self-concordant convex functions.

Proposition 1 Let $\hat{\mathbb{E}}$ and \mathbb{E} be finite-dimensional Euclidean spaces, and let $f(\hat{x}, s)$ be a nondegenerate α -self-concordant convex-concave function on $\hat{\mathbb{E}} \times \mathbb{E}$. Then the following properties hold:

- (i) For every $s \in \mathbb{E}$, $f(\cdot, s)$ is nondegenerate α -self-concordant on $\hat{\mathbb{E}}$, and for every $\hat{x} \in \hat{\mathbb{E}}$, $-f(\hat{x}, \cdot)$ is nondegenerate α -self-concordant on \mathbb{E} .

(ii) For every $w = (\hat{x}, s) \in \hat{\mathbb{E}} \times \mathbb{E}$ and $h_1, h_2, h_3 \in \hat{\mathbb{E}} \times \mathbb{E}$,

$$\left| D^3 f(w)[h_1, h_2, h_3] \right| \leq \frac{2}{\alpha^{1/2}} \prod_{i=1}^3 \sqrt{S_f(w)[h_i, h_i]}.$$

Proof The proof is provided in Appendix A.1. \square

Let f be a nondegenerate α -self-concordant convex-concave function on $\hat{\mathbb{E}} \times \mathbb{E}$. For any $w = (\hat{x}, s) \in \hat{\mathbb{E}} \times \mathbb{E}$ and any $h = (h_{\hat{x}}, h_s) \in \hat{\mathbb{E}} \times \mathbb{E}$, we define two local norms of h associated with f at w by

$$\|h\|_{f,w,\alpha} := \sqrt{\frac{1}{\alpha} S_f(w)[h, h]}, \quad \|h\|_{f,w,\alpha}^* := \sqrt{\frac{1}{\alpha} (S_f(w))^{-1}[h, h]}, \quad (12)$$

where $(S_f(w))^{-1}[h, h] := \langle h_{\hat{x}}, (D_{\hat{x}\hat{x}}^2 f(w))^{-1} h_{\hat{x}} \rangle - \langle h_s, (D_{ss}^2 f(w))^{-1} h_s \rangle$. Since α is fixed once f is specified, we omit it for brevity and write $\|h\|_{f,w}$ and $\|h\|_{f,w}^*$ as shorthand for $\|h\|_{f,w,\alpha}$ and $\|h\|_{f,w,\alpha}^*$, respectively.

We introduce three merit functions to measure how far the current iterate is from satisfying the optimality conditions. Specifically, let

$$\delta(w) := \|\Delta w\|_{f,w}, \quad \xi(w) := \|\nabla f(w)\|_{f,w}^*, \quad \theta(w) := \max_{\tilde{s}} f(\hat{x}, \tilde{s}) - \min_{\tilde{x}} f(\tilde{x}, s), \quad (13)$$

where $\Delta w := -(D^2 f(w))^{-1} \nabla f(w)$. Following the notation in [31], let $K(\theta) := \{w \mid \theta(w) < +\infty\}$. For $w \in K(\theta)$, the optimization problems $\max_{\tilde{s}} f(\hat{x}, \tilde{s})$ and $\min_{\tilde{x}} f(\tilde{x}, s)$ attain global optimal solutions, which are denoted by $s(\hat{x})$ and $\hat{x}(s)$, respectively. We further define the merit functions:

$$\tilde{\delta}_{\hat{x}}(w) = \sqrt{\frac{1}{\alpha} \langle \tilde{\Delta x}, D_{\hat{x}\hat{x}}^2 f(w) \tilde{\Delta x} \rangle}, \quad \tilde{\delta}_s(w) = \sqrt{-\frac{1}{\alpha} \langle \tilde{\Delta s}, D_{ss}^2 f(w) \tilde{\Delta s} \rangle}, \quad (14)$$

where $\tilde{\Delta x} := \hat{x} - \hat{x}(s)$ and $\tilde{\Delta s} := s - s(\hat{x})$. The connections among these merit functions are summarized in the following theorem.

Theorem 3 *Let $\hat{\mathbb{E}}$ and \mathbb{E} be finite-dimensional Euclidean spaces, and let $f : \hat{\mathbb{E}} \times \mathbb{E} \rightarrow \mathbb{R}$ be a nondegenerate α -self-concordant convex-concave function. For every $w = (\hat{x}, s) \in \hat{\mathbb{E}} \times \mathbb{E}$ and every $h = (h_{\hat{x}}, h_s) \in \hat{\mathbb{E}} \times \mathbb{E}$, the following statements hold:*

(i) If $r = \|\Delta w\|_{f,w} < 1$, then

$$(1-r)^2 S_f(w)[h, h] \leq S_f(w + \Delta w)[h, h] \leq \frac{1}{(1-r)^2} S_f(w)[h, h]. \quad (15)$$

(ii) $\delta(w) \leq \xi(w)$.

(iii) Let $w^+ := w + \Delta w \in \hat{\mathbb{E}} \times \mathbb{E}$. If $\delta(w) < 1$, then

$$\xi(w^+) \leq \left(\frac{\delta(w)}{1 - \delta(w)} \right)^2. \quad (16)$$

Furthermore, if $\delta(w) \leq \xi(w) \leq 2 - \sqrt{3}$, then $\xi(w^+) \leq \frac{\delta(w)}{2} \leq \frac{\xi(w)}{2}$.

(iv) If $\xi(w) < \frac{1}{3}$, then

$$\max\{\tilde{\delta}_{\hat{x}}(w), \tilde{\delta}_s(w)\} \leq 1 - (1 - 3\xi(w))^{\frac{1}{3}}. \quad (17)$$

Furthermore, if $\xi(w) \leq 0.1$, then $\max\{\tilde{\delta}_{\hat{x}}(w), \tilde{\delta}_s(w)\} < 0.2$.

Proof The proofs of (i)–(iii) follow directly from [31, Propositions 2.3 and 5.1]. The proof of (iv) is provided in Appendix A.2. \square

3 A minimax reformulation of the smoothing Newton method

In this section, we first reformulate the generalized parameterized smooth system as the first-order optimality conditions of a minimax problem. By eliminating the multiplier and the auxiliary variable, we obtain a reduced barrier augmented Lagrangian function η_ρ . We then show that η_ρ is a nondegenerate μ -self-concordant convex-concave function. Finally, we establish that the generalized parameterized smooth system is equivalent to the first-order optimality conditions of the minimax problem defined by η_ρ , and that the Newton system of SNM is equivalent to the corresponding Newton system for that minimax problem.

3.1 From the smoothing CHKS function to the reduced BAL function

We begin with the smoothing CHKS function

$$\Phi(x, s; \mu) = x + s - \left((x - s)^2 + 4\mu e \right)^{1/2},$$

and then introduce its generalized form Φ_ρ .

Given any point $(x, s) \in \mathbb{E} \times \mathbb{E}$ and $\mu > 0$, the classical SNM [13, 21, 29] based on Φ for problem (1) (inexactly) solves the parameterized smooth system

$$\mathcal{A}x = b, \mathcal{A}^*\lambda + s = c, \Phi(x, s; \mu) = 0. \quad (18)$$

Applying Newton's method to (18) yields the linearized system:

$$\begin{pmatrix} \mathcal{A} & 0 & 0 \\ 0 & \mathcal{I}_{\mathbb{E}} & \mathcal{A}^* \\ D_x\Phi(x, s; \mu) & D_s\Phi(x, s; \mu) & 0 \end{pmatrix} \begin{pmatrix} \Delta x \\ \Delta s \\ \Delta \lambda \end{pmatrix} = - \begin{pmatrix} \mathcal{A}x - b \\ \mathcal{A}^*\lambda + s - c \\ \Phi(x, s; \mu) \end{pmatrix}, \quad (19)$$

where $\mathcal{I}_{\mathbb{E}} : \mathbb{E} \rightarrow \mathbb{E}$ denotes the identity operator on \mathbb{E} . The classical SNM proceeds as follows. Starting from $(x^{(0)}, s^{(0)}, \lambda^{(0)})$, it computes the Newton direction given by (19), performs a line search along this direction at each iteration, and progressively decreases μ toward zero.

To generalize the parameterized smooth system, we derive an equivalent characterization of Φ . Let ϕ denote the natural barrier for \mathbb{K} . Given a fixed $\rho > 0$, consider the following optimization problem:

$$\min_{z \in \text{int}(\mathbb{K})} \left\{ \mu\phi(z) + \langle s, z \rangle + \frac{\rho}{2} \|z - x\|^2 \right\}. \quad (20)$$

Here ρ serves as the proximal regularization parameter in the quadratic term $\frac{\rho}{2} \|z - x\|^2$. For every fixed $\rho > 0$, the associated proximal problem (20) is well defined and admits a unique solution. The special choice $\rho = 1$ recovers the classical smoothing CHKS function, whereas allowing arbitrary $\rho > 0$ yields a family of smoothing CHKS-type functions.

The unique solution of (20) is the proximal point of the proper closed convex function $\mu\phi(\cdot) + \langle s, \cdot \rangle$ at x ; see [2, Theorem 6.3]. We denote this solution by $z_\rho(x, s; \mu)$. Then

$$z_\rho(x, s; \mu) = \frac{\rho x - s + \left((\rho x - s)^2 + 4\rho\mu e \right)^{1/2}}{2\rho} \in \text{int}(\mathbb{K}),$$

and satisfies the optimality condition

$$\mu \nabla \phi(z_\rho(x, s; \mu)) + s + \rho(z_\rho(x, s; \mu) - x) = 0. \quad (21)$$

Furthermore, $z_\rho(x, s; \mu)$ is a function of $(x, s; \mu) \in \mathbb{E} \times \mathbb{E} \times \mathbb{R}_{++}$. For brevity, we write z_ρ instead of $z_\rho(x, s; \mu)$ whenever no confusion arises. The natural generalization of Φ is then defined by

$$\Phi_\rho(x, s; \mu) := 2(x - z_\rho(x, s; \mu)), \quad \forall x, s \in \mathbb{E}, \mu > 0, \text{ and } \rho > 0. \quad (22)$$

In particular, $\Phi(x, s; \mu) = \Phi_1(x, s; \mu)$. The parameterized smooth system (18) generalizes to

$$\mathcal{A}x = b, \mathcal{A}^* \lambda + s = c, \Phi_\rho(x, s; \mu) = 0. \quad (23)$$

Applying Newton's method to (23) yields

$$\begin{pmatrix} \mathcal{A} & 0 & 0 \\ 0 & \mathcal{I}_{\mathbb{E}} & \mathcal{A}^* \\ D_x \Phi_\rho(x, s; \mu) & D_s \Phi_\rho(x, s; \mu) & 0 \end{pmatrix} \begin{pmatrix} \Delta x \\ \Delta s \\ \Delta \lambda \end{pmatrix} = - \begin{pmatrix} \mathcal{A}x - b \\ \mathcal{A}^* \lambda + s - c \\ \Phi_\rho(x, s; \mu) \end{pmatrix}. \quad (24)$$

The reformulation (23) extends the parameterized smooth system (18), with the classical smoothing CHKS function recovered as the special case $\rho = 1$. For simplicity, we continue to refer to the resulting method as an SNM.

We next show that (23) can be naturally related to a minimax problem, thereby further clarifying the optimization interpretation of Φ_ρ . Indeed, (23) is equivalent to

$$\mathcal{A}x = b, c - s + \frac{\rho}{2} \Phi_\rho(x, s; \mu) - \mathcal{A}^* \lambda = 0, \frac{1}{2} \Phi_\rho(x, s; \mu) = 0. \quad (25)$$

Combining (21), (22), and (25) yields the system

$$\mathcal{A}x = b, c - s - \rho(z - x) - \mathcal{A}^* \lambda = 0, z - x = 0, \mu \nabla \phi(z) + s + \rho(z - x) = 0.$$

This system is precisely the system of first-order optimality conditions of the following minimax problem, whose objective is the *barrier augmented Lagrangian* (BAL) function L_ρ :

$$\min_{z \in \text{int}(\mathbb{K}), x} \max_{s, \lambda} \{L_\rho(x, z, s, \lambda; \mu)\}, \quad (26)$$

where $L_\rho(x, z, s, \lambda; \mu) := \langle c, x \rangle + \mu \phi(z) - \langle \lambda, \mathcal{A}x - b \rangle + \langle s, z - x \rangle + \frac{\rho}{2} \|z - x\|^2$. The idea underlying the BAL function can be traced back to [26], and was further developed in [27, 28, 47, 48, 49].

Reformulation (26) reveals that the parameterized smooth system (23) can be interpreted as the first-order optimality conditions of the minimax problem (26). This suggests studying the SNM through the BAL function L_ρ . However, L_ρ is not suitable for direct self-concordant convex-concave analysis. Indeed, it is degenerate in both the multiplier λ and the s -variable, since $D_{\lambda\lambda}^2 L_\rho(x, z, s, \lambda; \mu) = 0$ and $D_{ss}^2 L_\rho(x, z, s, \lambda; \mu) = 0$. Therefore, we first restrict the formulation to the affine constraint $\mathcal{A}x = b$. Since \mathcal{A} is surjective, the linear system $\mathcal{A}x = b$ admits a solution for the given b . Fix an arbitrary feasible point \bar{x} such that $\mathcal{A}\bar{x} = b$. Let $\hat{\mathbb{E}}$ be a finite-dimensional Euclidean space such that $\dim \hat{\mathbb{E}} = \dim \ker \mathcal{A}$. Then there exists an injective linear operator $\mathcal{B} : \hat{\mathbb{E}} \rightarrow \mathbb{E}$ such that

$$\mathcal{A}\mathcal{B} = 0, \quad \mathcal{B}^* \mathcal{B} = \mathcal{I}_{\hat{\mathbb{E}}}.$$

Every feasible point x satisfying $\mathcal{A}x = b$ can be written uniquely as

$$x = \bar{x} + \mathcal{B}\hat{x}, \quad \hat{x} \in \hat{\mathbb{E}}.$$

Under this parametrization, the constraint term $-\langle \lambda, \mathcal{A}x - b \rangle$ vanishes identically, and the multiplier λ no longer appears. Thus, the degeneracy with respect to λ is removed.

We then eliminate the auxiliary variable z . This reduction also removes the degeneracy in the s -variable and leads to a reduced formulation suitable for a self-concordant convex-concave analysis. Define $\eta_\rho(\cdot, \cdot; \mu) : \hat{\mathbb{E}} \times \mathbb{E} \rightarrow \mathbb{R}$ by

$$\eta_\rho(\hat{x}, s; \mu) := \min_{z \in \text{int}(\mathbb{K})} \{L_\rho(\bar{x} + \mathcal{B}\hat{x}, z, s, \lambda; \mu)\}. \quad (27)$$

The value in $\eta_\rho(\hat{x}, s; \mu)$ is independent of λ , because $\mathcal{A}(\bar{x} + \mathcal{B}\hat{x}) = b$. Writing $x = \bar{x} + \mathcal{B}\hat{x}$, the unique minimizer in (27) is $z_\rho(x, s; \mu)$. Hence

$$\eta_\rho(\hat{x}, s; \mu) = \langle c, x \rangle + \mu\phi(z_\rho(x, s; \mu)) + \langle s, z_\rho(x, s; \mu) - x \rangle + \frac{\rho}{2}\|z_\rho(x, s; \mu) - x\|^2. \quad (28)$$

We call η_ρ the *reduced BAL* function. In the sequel, we write

$$w := (\hat{x}, s) \in \hat{\mathbb{E}} \times \mathbb{E}$$

for the reduced minimax variable whenever no confusion can arise. The resulting reduced minimax problem is

$$\min_{\hat{x} \in \hat{\mathbb{E}}} \max_{s \in \mathbb{E}} \{\eta_\rho(w; \mu)\}. \quad (29)$$

Compared with the original BAL function L_ρ , the reduced function η_ρ removes the affine multiplier degeneracy and, after eliminating z , has a nondegenerate curvature structure in both the minimization and maximization variables. These structural properties are established in the next subsection. In the remainder of the paper, we work with the reduced minimax problem (29) and the function η_ρ .

3.2 Properties of the reduced BAL function

In this subsection, we discuss the properties of the reduced BAL function η_ρ . Recall that $z_\rho(x, s; \mu)$ satisfies

$$\mu\nabla\phi(z_\rho(x, s; \mu)) + s + \rho(z_\rho(x, s; \mu) - x) = 0. \quad (30)$$

Define the adjoint variable associated with $z_\rho(x, s; \mu)$ by

$$y_\rho(x, s; \mu) := s + \rho(z_\rho(x, s; \mu) - x). \quad (31)$$

The variable $y_\rho(x, s; \mu)$ is also a function of $(x, s; \mu) \in \mathbb{E} \times \mathbb{E} \times \mathbb{R}_{++}$. Furthermore, both $z_\rho(x, s; \mu)$ and $y_\rho(x, s; \mu)$ satisfy the following properties.

Lemma 1 *For any scalars $\mu > 0$ and $\rho > 0$, the following statements are equivalent:*

$$(i) \ z_\rho(x, s; \mu) = x, \quad (ii) \ y_\rho(x, s; \mu) = s, \quad (iii) \ x, s \in \text{int}(\mathbb{K}), \ x \circ s = \mu e. \quad (32)$$

Proof The equivalence (i) \iff (ii) follows directly from the definition of $y_\rho(x, s; \mu)$. It suffices to prove that (i) \iff (iii).

Suppose that (iii) holds. By (30),

$$z_\rho(x, s; \mu) = \frac{\rho x - s + ((s - \rho x)^2 + 4\rho\mu e)^{1/2}}{2\rho}.$$

Since $x \circ s = \mu e$,

$$z_\rho(x, s; \mu) = \frac{\rho x - s + (s^2 - 2\rho s \circ x + \rho^2 x^2 + 4\rho\mu e)^{1/2}}{2\rho} = x,$$

which establishes (i).

Conversely, assume that (i) holds. By (30) and the inclusions $z_\rho, x \in \text{int}(\mathbb{K})$,

$$\mu \nabla \phi(x) + s = 0. \quad (33)$$

Combining (10) and (33) yields $s \in \text{int}(\mathbb{K})$ and $x \circ s = \mu e$. This establishes (iii) and completes the proof. \square

Define the linear operators

$$\mathcal{W} = \frac{\mu}{\rho} D^2 \phi(z_\rho(x, s; \mu)), \quad \mathcal{H} = \mathcal{I}_{\mathbb{E}} + \mathcal{W}. \quad (34)$$

Since the natural barrier ϕ is strictly convex on $\text{int}(\mathbb{K})$, we have

$$\mathcal{H} \succ \mathcal{W} \succ 0, \quad \mathcal{H} \succ \mathcal{I}_{\mathbb{E}}.$$

For brevity, all derivatives with respect to μ are denoted by a prime. For example, $z'_\rho(x, s; \mu) := D_\mu z_\rho(x, s; \mu)$. When no ambiguity arises, we also abbreviate $y_\rho(x, s; \mu)$ as y_ρ . The following theorem characterizes the derivatives of $z_\rho(x, s; \mu)$ and $y_\rho(x, s; \mu)$.

Theorem 4 *For any $\rho > 0$, the functions $z_\rho(x, s; \mu)$ and $y_\rho(x, s; \mu)$ are smooth with respect to (x, s, μ) on $\mathbb{E} \times \mathbb{E} \times \mathbb{R}_{++}$. Furthermore, their partial derivatives with respect to (x, s) are given by*

$$\begin{aligned} D_x z_\rho(x, s; \mu) &= \mathcal{H}^{-1}, & D_x y_\rho(x, s; \mu) &= -\rho \mathcal{H}^{-1} \mathcal{W}, \\ D_s z_\rho(x, s; \mu) &= -\rho^{-1} \mathcal{H}^{-1}, & D_s y_\rho(x, s; \mu) &= \mathcal{H}^{-1} \mathcal{W}, \end{aligned} \quad (35)$$

and the derivatives with respect to μ are given by

$$\begin{aligned} z'_\rho(x, s; \mu) &= -\rho^{-1} \mathcal{H}^{-1} \nabla \phi(z_\rho(x, s; \mu)), \\ y'_\rho(x, s; \mu) &= -\mathcal{H}^{-1} \nabla \phi(z_\rho(x, s; \mu)). \end{aligned} \quad (36)$$

Proof Recall that $\phi \in C^\infty(\text{int}(\mathbb{K}))$ and that $z_\rho(x, s; \mu)$ is defined as the unique solution to (30). Since

$$\mu D^2 \phi(z_\rho(x, s; \mu)) + \rho \mathcal{I}_{\mathbb{E}} = \rho \mathcal{H} \succ 0, \quad \forall (x, s, \mu) \in \mathbb{E} \times \mathbb{E} \times \mathbb{R}_{++}, \quad (37)$$

the derivative of the mapping

$$F_\rho(x, z, s; \mu) = \mu \nabla \phi(z) + s + \rho(z - x) \in C^\infty(\mathbb{E} \times \mathbb{E} \times \mathbb{E} \times \mathbb{R}_{++}, \mathbb{E})$$

with respect to z at $z = z_\rho(x, s; \mu)$ is nonsingular. Hence, the implicit function theorem implies $z_\rho \in C^\infty(\mathbb{E} \times \mathbb{E} \times \mathbb{R}_{++}, \mathbb{E})$. By definition,

$$y_\rho(x, s; \mu) = s + \rho(z_\rho(x, s; \mu) - x), \quad (38)$$

which implies that $y_\rho \in C^\infty(\mathbb{E} \times \mathbb{E} \times \mathbb{R}_{++}, \mathbb{E})$. Moreover, y_ρ satisfies

$$\mu \nabla \phi(z_\rho(x, s; \mu)) + y_\rho(x, s; \mu) = 0. \quad (39)$$

Differentiating both sides of (38) and (39) with respect to x yields

$$D_x y_\rho(x, s; \mu) = \rho(D_x z_\rho(x, s; \mu) - \mathcal{I}_{\mathbb{E}})$$

and

$$\mu D^2 \phi(z_\rho(x, s; \mu)) D_x z_\rho(x, s; \mu) + D_x y_\rho(x, s; \mu) = 0.$$

Consequently, we have

$$D_x z_\rho(x, s; \mu) = \rho(\mu D^2 \phi(z_\rho(x, s; \mu)) + \rho \mathcal{I}_{\mathbb{E}})^{-1} = \mathcal{H}^{-1}$$

and

$$\begin{aligned} D_x y_\rho(x, s; \mu) &= -\rho \left(\frac{\mu}{\rho} D^2 \phi(z_\rho(x, s; \mu)) + \mathcal{I}_{\mathbb{E}} \right)^{-1} \left(\frac{\mu}{\rho} D^2 \phi(z_\rho(x, s; \mu)) \right) \\ &= -\rho \mathcal{H}^{-1} \mathcal{W}. \end{aligned}$$

The remaining identities can be proved in the same way. \square

By Theorem 4 and (24), the search direction generated by the SNM is equivalently written as the solution of the linear system

$$\begin{pmatrix} \mathcal{A} & 0 & 0 \\ 0 & \mathcal{I}_{\mathbb{E}} & \mathcal{A}^* \\ \mathcal{H}^{-1} \mathcal{W} & \rho^{-1} \mathcal{H}^{-1} & 0 \end{pmatrix} \begin{pmatrix} \Delta x \\ \Delta s \\ \Delta \lambda \end{pmatrix} = - \begin{pmatrix} \mathcal{A}x - b \\ \mathcal{A}^* \lambda + s - c \\ x - z_\rho \end{pmatrix}. \quad (40)$$

The following proposition guarantees the uniqueness of this search direction.

Proposition 2 *For any point $(x, s, \lambda) \in \mathbb{E} \times \mathbb{E} \times \mathbb{R}^m$ and scalars $\mu > 0$, $\rho > 0$, the Newton system (40) generated by the SNM admits a unique solution.*

Proof The third equation in (40) gives

$$\Delta s = -\rho \mathcal{W} \Delta x - \rho \mathcal{H}(x - z_\rho).$$

Substituting this expression into the remaining equations, it suffices to verify the uniqueness of the solution to

$$\begin{pmatrix} -\rho \mathcal{W} & \mathcal{A}^* \\ \mathcal{A} & 0 \end{pmatrix} \begin{pmatrix} \Delta x \\ \Delta \lambda \end{pmatrix} = - \begin{pmatrix} \rho \mathcal{H}(z_\rho - x) + \mathcal{A}^* \lambda + s - c \\ \mathcal{A}x - b \end{pmatrix}. \quad (41)$$

Since $-\rho \mathcal{W}$ is invertible, the Schur complement of $\begin{pmatrix} -\rho \mathcal{W} & \mathcal{A}^* \\ \mathcal{A} & 0 \end{pmatrix}$ relative to $-\rho \mathcal{W}$ is $\rho^{-1} \mathcal{A} \mathcal{W}^{-1} \mathcal{A}^*$. Moreover, $\mathcal{W}^{-1} \succ 0$ and \mathcal{A} is surjective. Therefore, $\rho^{-1} \mathcal{A} \mathcal{W}^{-1} \mathcal{A}^*$ is invertible and the system (41) admits a unique solution. \square

The next corollary provides explicit formulas for the first- and second-order derivatives of $\eta_\rho(w; \mu)$ with respect to \hat{x} and s .

Corollary 1 For any $\rho > 0$, the reduced BAL function $\eta_\rho(w; \mu)$ is smooth on $\hat{\mathbb{E}} \times \mathbb{E} \times \mathbb{R}_{++}$. Furthermore, for $x = \bar{x} + \mathcal{B}\hat{x}$,

$$\nabla_{\hat{x}}\eta_\rho(w; \mu) = \mathcal{B}^*(c - y_\rho(x, s; \mu)), \quad \nabla_s\eta_\rho(w; \mu) = z_\rho(x, s; \mu) - x, \quad (42)$$

and

$$\begin{aligned} D_{\hat{x}\hat{x}}^2\eta_\rho(w; \mu) &= \rho\mathcal{B}^*\mathcal{H}^{-1}\mathcal{W}\mathcal{B}, & D_{ss}^2\eta_\rho(w; \mu) &= -\rho^{-1}\mathcal{H}^{-1}, \\ D_{\hat{x}s}^2\eta_\rho(w; \mu) &= -\mathcal{B}^*\mathcal{H}^{-1}\mathcal{W}, & D_{s\hat{x}}^2\eta_\rho(w; \mu) &= -\mathcal{H}^{-1}\mathcal{W}\mathcal{B}. \end{aligned} \quad (43)$$

Proof The smoothness of η_ρ follows immediately from Theorem 4. By differentiating (27) with respect to \hat{x} and using the chain rule, we obtain

$$\begin{aligned} \nabla_{\hat{x}}\eta_\rho(w; \mu) &= \mathcal{B}^*(\nabla_x\eta_\rho(w; \mu)) \\ &= \mathcal{B}^*(c + \mu D_x z_\rho(x, s; \mu)\nabla\phi(z_\rho(x, s; \mu)) \\ &\quad + (D_x z_\rho(x, s; \mu) - \mathcal{I}_{\mathbb{E}})(s + \rho(z_\rho(x, s; \mu) - x))). \end{aligned}$$

By (30) and (31), we have

$$\begin{aligned} \nabla_{\hat{x}}\eta_\rho(w; \mu) &= \mathcal{B}^*(D_x z_\rho(x, s; \mu)(\mu\nabla\phi(z_\rho(x, s; \mu)) + y_\rho(x, s; \mu)) \\ &\quad + c - y_\rho(x, s; \mu)) \\ &= \mathcal{B}^*(c - y_\rho(x, s; \mu)). \end{aligned} \quad (44)$$

Further differentiating (44) with respect to \hat{x} yields

$$D_{\hat{x}\hat{x}}^2\eta_\rho(w; \mu) = \rho\mathcal{B}^*\mathcal{H}^{-1}\mathcal{W}\mathcal{B}.$$

The remaining identities follow by analogous arguments. \square

Corollary 1 implies that $\eta_\rho(w; \mu)$ is convex in \hat{x} and concave in s . The following theorem further shows that $\eta_\rho(w; \mu)$ is a nondegenerate μ -self-concordant convex-concave function.

Theorem 5 For any $\mu > 0$ and $\rho > 0$, the reduced BAL function $\eta_\rho(\cdot, \cdot; \mu)$ is a nondegenerate μ -self-concordant convex-concave function on $\hat{\mathbb{E}} \times \mathbb{E}$. Furthermore, $\eta_\rho(\cdot, s; \mu)$ is nondegenerate μ -self-concordant on $\hat{\mathbb{E}}$ for every $s \in \mathbb{E}$, and $-\eta_\rho(\hat{x}, \cdot; \mu)$ is nondegenerate μ -self-concordant on \mathbb{E} for every $\hat{x} \in \hat{\mathbb{E}}$.

Proof The smoothness of η_ρ follows from Corollary 1. For any $h = (h_{\hat{x}}, h_s) \in \hat{\mathbb{E}} \times \mathbb{E}$,

$$S_{\eta_\rho}(w; \mu)[h, h] = \rho\langle h_{\hat{x}}, \mathcal{B}^*\mathcal{H}^{-1}\mathcal{W}\mathcal{B}h_{\hat{x}} \rangle + \rho^{-1}\langle h_s, \mathcal{H}^{-1}h_s \rangle.$$

Since \mathcal{B} is injective and $\mathcal{H}^{-1}\mathcal{W} \succ 0$, the operator $\mathcal{B}^*\mathcal{H}^{-1}\mathcal{W}\mathcal{B}$ is positive definite on $\hat{\mathbb{E}}$. Combined with $\mathcal{H}^{-1} \succ 0$, this shows that $S_{\eta_\rho}(w; \mu)$ is positive definite, so $\eta_\rho(w; \mu)$ is nondegenerate. By Definition 3, it suffices to prove that

$$|D^3\eta_\rho(w; \mu)[h, h, h]| \leq \frac{2}{\sqrt{\mu}}(S_{\eta_\rho}(w; \mu)[h, h])^{3/2}.$$

Let $\bar{h} = (\bar{h}_x, \bar{h}_s) = (\mathcal{H}^{-1}\mathcal{B}h_{\hat{x}}, \mathcal{H}^{-1}h_s) \in \mathbb{E} \times \mathbb{E}$. By Corollary 1 and the formula $\mathcal{H} = \mathcal{I}_{\mathbb{E}} + \mathcal{W} = \mathcal{I}_{\mathbb{E}} + \frac{\mu}{\rho}D^2\phi(z_\rho)$, we have

$$\begin{aligned}
& S_{\eta_\rho}(w; \mu)[h, h] \\
&= \rho \langle \bar{h}_x, \mathcal{H}\mathcal{W}\bar{h}_x \rangle + \rho^{-1} \langle \bar{h}_s, \mathcal{H}\bar{h}_s \rangle \\
&= \mu D^2\phi(z_\rho)[\bar{h}_x, \bar{h}_x] + \frac{\mu^2}{\rho} \|D^2\phi(z_\rho)\bar{h}_x\|^2 + \rho^{-1} \|\bar{h}_s\|^2 + \frac{\mu}{\rho^2} D^2\phi(z_\rho)[\bar{h}_s, \bar{h}_s] \quad (45) \\
&= \mu D^2\phi(z_\rho)[\bar{h}_x - \rho^{-1}\bar{h}_s, \bar{h}_x - \rho^{-1}\bar{h}_s] + \frac{1}{\rho} \|\mu D^2\phi(z_\rho)\bar{h}_x + \bar{h}_s\|^2 \\
&\geq \mu D^2\phi(z_\rho)[\bar{h}_x - \rho^{-1}\bar{h}_s, \bar{h}_x - \rho^{-1}\bar{h}_s],
\end{aligned}$$

and

$$\begin{aligned}
D^2\eta_\rho(w; \mu)[h, h] &= \rho \langle \mathcal{B}h_{\hat{x}}, (\mathcal{I}_{\mathbb{E}} - \mathcal{H}^{-1})\mathcal{B}h_{\hat{x}} \rangle - \rho^{-1} \langle h_s, \mathcal{H}^{-1}h_s \rangle \\
&\quad + 2 \langle \mathcal{B}h_{\hat{x}}, (\mathcal{H}^{-1} - \mathcal{I}_{\mathbb{E}})h_s \rangle.
\end{aligned}$$

A direct calculation gives

$$D_{\hat{x}}\mathcal{H}^{-1}[h_{\hat{x}}, \cdot, \cdot] = -\frac{\mu}{\rho}D^3\phi(z_\rho)[\bar{h}_x, \mathcal{H}^{-1}\cdot, \mathcal{H}^{-1}\cdot], \quad (46a)$$

$$D_s\mathcal{H}^{-1}[h_s, \cdot, \cdot] = \frac{\mu}{\rho^2}D^3\phi(z_\rho)[\bar{h}_s, \mathcal{H}^{-1}\cdot, \mathcal{H}^{-1}\cdot]. \quad (46b)$$

Thus, we have

$$\begin{aligned}
& D^3\eta_\rho(w; \mu)[h, h, h] \\
&= -\rho D_{\hat{x}}\mathcal{H}^{-1}[h_{\hat{x}}, \mathcal{B}h_{\hat{x}}, \mathcal{B}h_{\hat{x}}] - \rho D_s\mathcal{H}^{-1}[h_s, \mathcal{B}h_{\hat{x}}, \mathcal{B}h_{\hat{x}}] \\
&\quad - \rho^{-1} D_{\hat{x}}\mathcal{H}^{-1}[h_{\hat{x}}, h_s, h_s] - \rho^{-1} D_s\mathcal{H}^{-1}[h_s, h_s, h_s] \\
&\quad + 2D_{\hat{x}}\mathcal{H}^{-1}[h_{\hat{x}}, \mathcal{B}h_{\hat{x}}, h_s] + 2D_s\mathcal{H}^{-1}[h_s, \mathcal{B}h_{\hat{x}}, h_s] \\
&= \mu D^3\phi(z_\rho)[\bar{h}_x - \rho^{-1}\bar{h}_s, \bar{h}_x - \rho^{-1}\bar{h}_s, \bar{h}_x - \rho^{-1}\bar{h}_s].
\end{aligned}$$

Taking absolute values and using the standard self-concordance of ϕ , we obtain

$$\begin{aligned}
\left| D^3\eta_\rho(w; \mu)[h, h, h] \right| &= \mu \left| D^3\phi(z_\rho)[\bar{h}_x - \rho^{-1}\bar{h}_s, \bar{h}_x - \rho^{-1}\bar{h}_s, \bar{h}_x - \rho^{-1}\bar{h}_s] \right| \\
&\leq 2\mu \left\{ D^2\phi(z_\rho)[\bar{h}_x - \rho^{-1}\bar{h}_s, \bar{h}_x - \rho^{-1}\bar{h}_s] \right\}^{3/2} \\
&\leq \frac{2}{\sqrt{\mu}} (S_{\eta_\rho}(w; \mu)[h, h])^{3/2},
\end{aligned}$$

where the second inequality follows from (45). Hence, $\eta_\rho(\cdot, \cdot; \mu)$ is a nondegenerate μ -self-concordant convex-concave function on $\hat{\mathbb{E}} \times \mathbb{E}$. The remaining statements follow immediately from Proposition 1. \square

3.3 Equivalent characterization of the parameterized smooth system

This subsection establishes the key equivalence between the parameterized smooth system (23) and the first-order optimality conditions of the minimax problem (29).

We begin by recalling the barrier subproblem arising in IPMs:

$$\min \{ \langle c, x \rangle + \mu \phi(x) \mid \mathcal{A}x = b, x \in \text{int}(\mathbb{K}) \}. \quad (47)$$

The following lemma establishes the connection between (23) and (47).

Lemma 2 *For any $\mu > 0$ and $\rho > 0$, the triple $(x(\mu), s(\mu), \lambda(\mu))$ solves the parameterized smooth system (23) if and only if it is the KKT triple of the barrier subproblem (47).*

Proof By definition, the triple $(x(\mu), s(\mu), \lambda(\mu))$ solves (23) if and only if it satisfies

$$\mathcal{A}x(\mu) - b = 0, \mathcal{A}^* \lambda(\mu) + s(\mu) - c = 0, \Phi_\rho(x(\mu), s(\mu); \mu) = 0.$$

Since $\Phi_\rho(x(\mu), s(\mu); \mu) = 2(x(\mu) - z_\rho(x(\mu), s(\mu); \mu))$, it follows from Lemma 1 that

$$\mathcal{A}x(\mu) = b, \mathcal{A}^* \lambda(\mu) + s(\mu) - c = 0, x(\mu), s(\mu) \in \text{int}(\mathbb{K}), x(\mu) \circ s(\mu) = \mu e.$$

Consequently, $(x(\mu), s(\mu), \lambda(\mu))$ is the KKT triple associated with the barrier subproblem (47). The converse implication follows by reversing the above arguments, and the proof is complete. \square

Based on Lemma 2, we now establish the equivalence between the parameterized smooth system (23) and the first-order optimality conditions of the minimax problem (29).

Theorem 6 *For any $\mu > 0$ and $\rho > 0$, suppose that $(x(\mu), s(\mu), \lambda(\mu))$ solves the parameterized smooth system (23). Then the pair $(\hat{x}(\mu), s(\mu)) := (\mathcal{B}^*(x(\mu) - \bar{x}), s(\mu))$ is a saddle point of the minimax problem (29). Conversely, if $(\hat{x}(\mu), s(\mu))$ is a saddle point of (29), then*

$$(x(\mu), s(\mu), \lambda(\mu)) := (\bar{x} + \mathcal{B}\hat{x}(\mu), s(\mu), (\mathcal{A}\mathcal{A}^*)^{-1} \mathcal{A}(c - s(\mu)))$$

solves the parameterized smooth system (23).

Proof Suppose that the triple $(x(\mu), s(\mu), \lambda(\mu))$ solves (23). By Lemma 2, we have

$$\mathcal{A}x(\mu) = b, \mathcal{A}^* \lambda(\mu) + s(\mu) - c = 0, x(\mu), s(\mu) \in \text{int}(\mathbb{K}), x(\mu) \circ s(\mu) = \mu e. \quad (48)$$

Together with Lemma 1, this yields

$$z_\rho(x(\mu), s(\mu); \mu) = x(\mu).$$

Thus, it follows from Corollary 1 that

$$\nabla_s \eta_\rho(\hat{x}(\mu), s(\mu); \mu) = z_\rho(x(\mu), s(\mu); \mu) - x(\mu) = 0.$$

Furthermore,

$$\begin{aligned} \nabla_{\hat{x}} \eta_\rho(\hat{x}(\mu), s(\mu); \mu) &= \mathcal{B}^*(c - y_\rho(x(\mu), s(\mu); \mu)) \\ &= \mathcal{B}^*(c - s(\mu) - \rho(z_\rho(x(\mu), s(\mu); \mu) - x(\mu))). \end{aligned}$$

By the identity $z_\rho(x(\mu), s(\mu); \mu) = x(\mu)$ and the second equation in (48), we have

$$\nabla_{\hat{x}} \eta_\rho(\hat{x}(\mu), s(\mu); \mu) = \mathcal{B}^*(c - s(\mu)) = \mathcal{B}^* \mathcal{A}^* \lambda(\mu) = 0.$$

Therefore, $(\hat{x}(\mu), s(\mu)) := (\mathcal{B}^*(x(\mu) - \bar{x}), s(\mu))$ satisfies the first-order optimality conditions of the minimax problem (29). Since η_ρ is convex-concave, this pair is a saddle point of (29).

Conversely, suppose that $(\hat{x}(\mu), s(\mu))$ is a saddle point of (29). Then it satisfies

$$z_\rho(x(\mu), s(\mu); \mu) = x(\mu), \mathcal{B}^*(c - y_\rho(x(\mu), s(\mu); \mu)) = 0, \quad (49)$$

where $x(\mu) = \bar{x} + \mathcal{B}\hat{x}(\mu)$. By Lemma 1, we have

$$x(\mu), s(\mu) \in \text{int}(\mathbb{K}), \quad x(\mu) \circ s(\mu) = \mu e,$$

and $\mathcal{A}x(\mu) - b = \mathcal{A}\bar{x} - b + \mathcal{A}\mathcal{B}\hat{x}(\mu) = 0$. It remains to show that

$$\mathcal{A}^* \lambda(\mu) + s(\mu) - c = 0.$$

Note that the second equation of (49) implies

$$c - y_\rho(x(\mu), s(\mu); \mu) = c - s(\mu) \in (\ker \mathcal{A})^\perp.$$

Since \mathcal{A} is surjective and $\mathcal{A}^*(\mathcal{A}\mathcal{A}^*)^{-1}\mathcal{A}$ is the orthogonal projector onto $(\ker \mathcal{A})^\perp$, we obtain

$$\mathcal{A}^* \lambda(\mu) + s(\mu) - c = (\mathcal{I}_{\mathbb{E}} - \mathcal{A}^*(\mathcal{A}\mathcal{A}^*)^{-1}\mathcal{A})(s(\mu) - c) = 0,$$

which concludes the proof. \square

Remark 2 According to [34, Theorem 4.1], the barrier subproblem (47) admits a unique primal-dual optimal solution. Together with Theorem 6, this implies that the minimax problem (29) admits a unique saddle point for any $\mu > 0$ and $\rho > 0$.

The following theorem characterizes the search direction of the SNM.

Theorem 7 *Let (x, s, λ) satisfy the affine constraint $\mathcal{A}x = b$. For any scalars $\mu > 0$ and $\rho > 0$, suppose that $(\Delta x, \Delta s, \Delta \lambda)$ is the search direction generated by the SNM, satisfying (40). Then the pair $(\Delta \hat{x}, \Delta s) := (\mathcal{B}^* \Delta x, \Delta s)$ is the unique Newton direction for the minimax problem (29), given by*

$$\begin{pmatrix} \rho \mathcal{B}^* \mathcal{H}^{-1} \mathcal{W} \mathcal{B} & -\mathcal{B}^* \mathcal{H}^{-1} \mathcal{W} \\ -\mathcal{H}^{-1} \mathcal{W} \mathcal{B} & -\rho^{-1} \mathcal{H}^{-1} \end{pmatrix} \begin{pmatrix} \Delta \hat{x} \\ \Delta s \end{pmatrix} = - \begin{pmatrix} \mathcal{B}^*(c - y_\rho) \\ z_\rho - x \end{pmatrix}. \quad (50)$$

Conversely, suppose that $(\Delta \hat{x}, \Delta s)$ is the Newton direction for the minimax problem (29). Define

$$\Delta \lambda := (\mathcal{A}\mathcal{A}^*)^{-1} \mathcal{A}(-s - \Delta s + c - \mathcal{A}^* \lambda). \quad (51)$$

Then $(\Delta x, \Delta s, \Delta \lambda) = (\mathcal{B}\Delta \hat{x}, \Delta s, \Delta \lambda)$ is the unique search direction given by the SNM.

Proof Suppose that $(\Delta x, \Delta s, \Delta \lambda)$ is the search direction generated by the SNM. Let $(\Delta \hat{x}, \Delta s) = (\mathcal{B}^* \Delta x, \Delta s)$. We first show that $\Delta x = \mathcal{B} \Delta \hat{x}$. Since $\mathcal{A} \Delta x = -(\mathcal{A}x - b) = 0$, there exists a unique vector $\Delta \bar{x} \in \mathbb{E}$ such that $\Delta x = \mathcal{B} \Delta \bar{x}$. It follows that

$$\Delta \hat{x} = \mathcal{B}^* \Delta x = \mathcal{B}^* \mathcal{B} \Delta \bar{x} = \Delta \bar{x}.$$

Thus, $\Delta \hat{x} = \Delta \bar{x}$ and $\Delta x = \mathcal{B} \Delta \hat{x}$. Consequently,

$$\begin{aligned} & \rho \mathcal{B}^* \mathcal{H}^{-1} \mathcal{W} \mathcal{B} \Delta \hat{x} - \mathcal{B}^* \mathcal{H}^{-1} \mathcal{W} \Delta s + \mathcal{B}^* (c - y_\rho) \\ &= \mathcal{B}^* (\rho \mathcal{H}^{-1} \mathcal{W} \Delta x - \mathcal{H}^{-1} \mathcal{W} \Delta s + c - s - \rho(z_\rho - x)) \\ &= \mathcal{B}^* (c - s - \Delta s) \\ &= \mathcal{B}^* \mathcal{A}^* (\lambda + \Delta \lambda) \\ &= 0. \end{aligned}$$

Here the second and third equalities follow from the third and second equations of (40), respectively. The second equation of (50) follows directly from the third equation of (40). Consequently, the linear system (50) admits at least one solution. Since the Schur complement of the operator in (50) relative to $-\rho^{-1} \mathcal{H}^{-1}$ is $\rho \mathcal{B}^* \mathcal{W} \mathcal{B} \succ 0$, the uniqueness follows directly.

Conversely, suppose that $(\Delta \hat{x}, \Delta s)$ is the Newton direction for the minimax problem (29). Then,

$$\mathcal{A} \Delta x = \mathcal{A} \mathcal{B} \Delta \hat{x} = 0 = -(\mathcal{A}x - b),$$

so the first equation of (40) holds. Furthermore, the second block row of (50) gives

$$-\mathcal{H}^{-1} \mathcal{W} \mathcal{B} \Delta \hat{x} - \rho^{-1} \mathcal{H}^{-1} \Delta s = -(z_\rho - x).$$

Since $\Delta x = \mathcal{B} \Delta \hat{x}$, this is equivalent to

$$\mathcal{H}^{-1} \mathcal{W} \Delta x + \rho^{-1} \mathcal{H}^{-1} \Delta s = z_\rho - x,$$

which is precisely the third equation of (40). It remains to verify the second equation of (40). Multiplying the second equation in (50) on the left by $\rho \mathcal{B}^*$ and adding it to the first equation, we obtain

$$\mathcal{B}^* (c - s - \Delta s) = 0.$$

This implies $s + \Delta s - c \in (\ker \mathcal{A})^\perp$. Combined with (51),

$$\mathcal{A}^* (\lambda + \Delta \lambda) + s + \Delta s - c = (\mathcal{I}_{\mathbb{E}} - \mathcal{A}^* (\mathcal{A} \mathcal{A}^*)^{-1} \mathcal{A}) (s + \Delta s - c).$$

Since $\mathcal{I}_{\mathbb{E}} - \mathcal{A}^* (\mathcal{A} \mathcal{A}^*)^{-1} \mathcal{A}$ is the orthogonal projection onto $\ker \mathcal{A}$, we have

$$\mathcal{A}^* (\lambda + \Delta \lambda) + s + \Delta s - c = 0.$$

Thus all three equations in (40) are satisfied. The uniqueness of $(\Delta x, \Delta s, \Delta \lambda)$ follows from Proposition 2, and the proof is complete. \square

Theorems 6 and 7 provide an equivalent characterization of both the parameterized smooth system and the search direction generated by the SNM via the reduced BAL function η_ρ . This equivalence implies that, in the subsequent algorithmic analysis, it suffices to study the Newton iterations applied to the minimax

problem (29). This offers a convenient and powerful tool for analyzing the behavior of the SNM. We conclude this section with a summary of the main characterizations obtained.

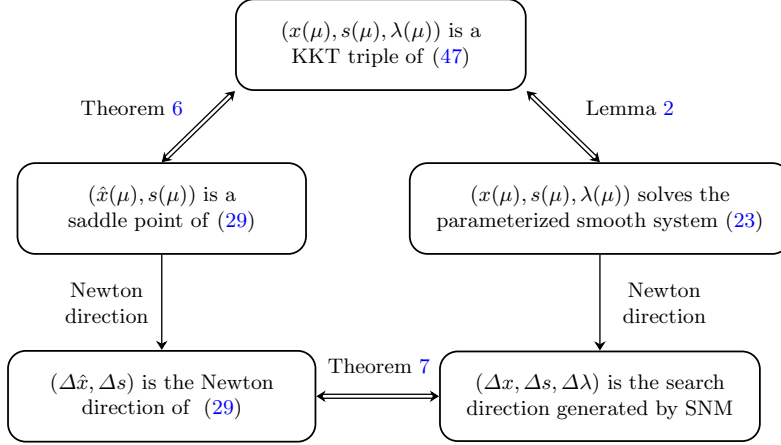


Fig. 1: Summary of equivalence relationships

4 A path-following smoothing Newton method

This section proposes a path-following smoothing Newton method for symmetric cone programming. The method consists of two phases. In the first phase, an initial point is constructed in a well-defined neighborhood of the central path. The second phase then uses this point to generate iterates that remain in the neighborhood and terminates once the prescribed accuracy is reached.

4.1 Neighborhood of the central path

For both practical implementation and theoretical analysis, maintaining iterates within a well-defined neighborhood of the central path is critical. To measure the proximity of a point to the central path and drive the iteration process, we introduce several auxiliary merit functions.

By Theorem 5, the function $\eta_\rho(w; \mu)$ is strictly convex in $\hat{x} \in \hat{\mathbb{E}}$ and strictly concave in $s \in \mathbb{E}$. Accordingly, we measure its suboptimality by the primal-dual gap function as in (13):

$$\begin{aligned} \theta_\rho(w; \mu) &= \max_{\tilde{s}} \eta_\rho(\hat{x}, \tilde{s}; \mu) - \min_{\tilde{x}} \eta_\rho(\tilde{x}, s; \mu) \\ &= \eta_\rho(\hat{x}, s_\rho(\hat{x}, \mu); \mu) - \eta_\rho(\hat{x}_\rho(s, \mu), s; \mu), \end{aligned} \quad (52)$$

where $s_\rho(\hat{x}, \mu) = \arg \max_{\tilde{s}} \eta_\rho(\hat{x}, \tilde{s}; \mu)$, $\hat{x}_\rho(s, \mu) = \arg \min_{\tilde{x}} \eta_\rho(\tilde{x}, s; \mu)$.

Let $(\hat{x}(\mu), s(\mu))$ be the saddle point of the minimax problem (29), which always exists for any $\mu > 0$ and $\rho > 0$ by Remark 2. Then for any $(\hat{x}, s) \in \hat{\mathbb{E}} \times \mathbb{E}$, the following inequalities hold:

$$\max_{\tilde{s}} \eta_{\rho}(\hat{x}, \tilde{s}; \mu) \geq \eta_{\rho}(\hat{x}(\mu), s(\mu); \mu) \geq \min_{\tilde{x}} \eta_{\rho}(\tilde{x}, s; \mu). \quad (53)$$

Let $\text{val}(P_{\mu})$ denote the optimal value of the barrier problem (47). By Theorem 6,

$$\eta_{\rho}(\hat{x}(\mu), s(\mu); \mu) = \text{val}(P_{\mu}).$$

Combining this with (53) yields that, for any $(\hat{x}, s) \in \hat{\mathbb{E}} \times \mathbb{E}$,

$$|\eta_{\rho}(w; \mu) - \text{val}(P_{\mu})| \leq \theta_{\rho}(w; \mu). \quad (54)$$

Furthermore, (53) implies that $\theta_{\rho}(w; \mu) \geq 0$, and $\theta_{\rho}(w; \mu) = 0$ holds if and only if (\hat{x}, s) is the saddle point of (29). This gap therefore provides a certificate of optimality and will be used to measure the proximity to the central path.

In practice, evaluating the exact primal-dual gap $\theta_{\rho}(w; \mu)$ is computationally prohibitive, as it requires solving optimization problems. Recall that $x = \bar{x} + \mathcal{B}\hat{x}$. Let $(\Delta x, \Delta s, \Delta \lambda)$ be the search direction given by (40), and let $\Delta w = (\Delta \hat{x}, \Delta s)$ be the Newton direction for the minimax problem (29). For algorithmic purposes, we follow (13) and introduce easily computable merit functions:

$$\delta_{\hat{x}, \rho}(w; \mu) = \sqrt{\frac{1}{\mu} \langle \Delta \hat{x}, D_{\hat{x}\hat{x}}^2 \eta_{\rho}(w; \mu) \Delta \hat{x} \rangle}, \quad (55a)$$

$$\delta_{s, \rho}(w; \mu) = \sqrt{-\frac{1}{\mu} \langle \Delta s, D_{ss}^2 \eta_{\rho}(w; \mu) \Delta s \rangle}, \quad (55b)$$

$$\delta_{\rho}(w; \mu) = \sqrt{(\delta_{\hat{x}, \rho}(w; \mu))^2 + (\delta_{s, \rho}(w; \mu))^2} = \|\Delta w\|_{\eta_{\rho}, w}, \quad (55c)$$

$$\xi_{\hat{x}, \rho}(w; \mu) = \sqrt{\frac{1}{\mu} \langle \nabla_{\hat{x}} \eta_{\rho}(w; \mu), (D_{\hat{x}\hat{x}}^2 \eta_{\rho}(w; \mu))^{-1} \nabla_{\hat{x}} \eta_{\rho}(w; \mu) \rangle}, \quad (55d)$$

$$\xi_{s, \rho}(w; \mu) = \sqrt{-\frac{1}{\mu} \langle \nabla_s \eta_{\rho}(w; \mu), (D_{ss}^2 \eta_{\rho}(w; \mu))^{-1} \nabla_s \eta_{\rho}(w; \mu) \rangle}, \quad (55e)$$

$$\xi_{\rho}(w; \mu) = \sqrt{(\xi_{\hat{x}, \rho}(w; \mu))^2 + (\xi_{s, \rho}(w; \mu))^2} = \|\nabla_w \eta_{\rho}(w; \mu)\|_{\eta_{\rho}, w}^*. \quad (55f)$$

These quantities serve as surrogate measures of the quality of the current iterate.

Remark 3 By Corollary 1, we have

$$\delta_{\hat{x}, \rho}(w; \mu) = \sqrt{\frac{1}{\mu} \langle \Delta x, D_{xx}^2 \eta_{\rho}(w; \mu) \Delta x \rangle}.$$

This implies that it is unnecessary to explicitly form $\Delta \hat{x}$ and $\nabla_{\hat{x}\hat{x}}^2 \eta_{\rho}(w; \mu)$ in practical computations. The quantity $\delta_{\hat{x}, \rho}(w; \mu)$ can be computed directly from Δx and $D_{xx}^2 \eta_{\rho}(w; \mu)$.

If $\xi_{\rho}(w; \mu) = 0$, then (\hat{x}, s) is the saddle point of the minimax problem (29). This defines a central path that coincides with the one generated by IPMs, as shown in Theorem 6. Specifically,

$$\begin{aligned} & \mathcal{A}x = b, \mathcal{A}^* \lambda + s = c, x \in \text{int}(\mathbb{K}), s \in \text{int}(\mathbb{K}), x \circ s = \mu e \\ \iff & \mathcal{A}x = b, \mathcal{A}^* \lambda + s = c, \xi_{\rho}(w; \mu) = 0. \end{aligned} \quad (56)$$

Motivated by this equivalence, we define the central-path neighborhood for the SNM based on the reduced BAL function η_ρ by

$$\mathcal{N}(\kappa, \mu, \rho) := \{(x, s, \lambda) \in \mathbb{E} \times \mathbb{E} \times \mathbb{R}^m \mid \mathcal{A}x = b, \mathcal{A}^*\lambda + s = c, \xi_\rho(w; \mu) \leq \kappa\}, \quad (57)$$

where $\kappa = 0.1$ is fixed throughout the algorithm and the complexity analysis.

This neighborhood differs from the standard neighborhoods used in classical interior-point path-following methods [30, 34, 38] or in non-interior path-following methods [4, 5, 8, 50]. It is defined via the merit function induced by the minimax problem, and is tailored to the structure of the SNM. The proposed method follows the standard paradigm of path-following methods. In the first phase, the iterates are driven into $\mathcal{N}(\kappa, \mu^{(0)}, \rho)$. In the second phase, the iterates are maintained in $\mathcal{N}(\kappa, \mu^{(k)}, \rho)$ while the smoothing parameter is updated.

4.2 Two-phase path-following framework

Before introducing the two-phase framework, we present some additional notation. Let

$$v := (x, s, \lambda), \quad \Delta v := (\Delta x, \Delta s, \Delta \lambda).$$

Define $K(\theta_\rho) := \{w \mid \theta_\rho(w; \mu) < +\infty\}$. For a given initial point $w^{(0,0)} := (\hat{x}^{(0,0)}, s^{(0,0)}) \in K(\theta_\rho)$, let $\bar{x} \in \mathbb{E}$ satisfy $\mathcal{A}\bar{x} = b$, and set

$$x^{(0,0)} = \bar{x} + \mathcal{B}\hat{x}^{(0,0)}.$$

For $t \in (0, 1]$, define the perturbed function

$$\eta_{t,\rho}(w; \mu^{(0)}) := \eta_\rho(w; \mu^{(0)}) - t \langle \nabla_w \eta_\rho(w^{(0,0)}; \mu^{(0)}), w \rangle. \quad (58)$$

The purpose of this perturbation is to construct a continuation path from the initial point to a point satisfying the neighborhood condition for the fixed parameter $\mu^{(0)}$. Since η_ρ is a nondegenerate μ -self-concordant convex-concave function, $\eta_{t,\rho}$ inherits the same property for any $t \geq 0$.

The first phase of PFSNM aims to generate a feasible point in the neighborhood $\mathcal{N}(\kappa, \mu^{(0)}, \rho)$. The parameter t scales the perturbation term so that the initial point $(x^{(0,0)}, s^{(0,0)}, \lambda^{(0,0)})$ lies in the central-path neighborhood of the perturbed problem. For this purpose, consider the minimax problem

$$\min_{\hat{x} \in \hat{\mathbb{E}}} \max_{s \in \mathbb{E}} \left\{ \eta_{t,\rho}(w; \mu^{(0)}) \right\}$$

with the first-order optimality conditions

$$\begin{aligned} \mathcal{B}^*(c - y_\rho) - t\mathcal{B}^*(c - y_\rho^{(0,0)}) &= 0, \\ z_\rho - x - t(z_\rho^{(0,0)} - x^{(0,0)}) &= 0, \end{aligned} \quad (59)$$

where $y_\rho^{(0,0)} := y_\rho(w^{(0,0)}; \mu^{(0)})$ and $z_\rho^{(0,0)} := z_\rho(w^{(0,0)}; \mu^{(0)})$.

Applying Newton's method to the nonlinear system (59) leads to the search direction $(\Delta \hat{x}, \Delta s)$ satisfying

$$\begin{pmatrix} \rho \mathcal{B}^* \mathcal{H}^{-1} \mathcal{W} \mathcal{B} & -\mathcal{B}^* \mathcal{H}^{-1} \mathcal{W} \\ -\mathcal{H}^{-1} \mathcal{W} \mathcal{B} & -\rho^{-1} \mathcal{H}^{-1} \end{pmatrix} \begin{pmatrix} \Delta \hat{x} \\ \Delta s \end{pmatrix} = - \begin{pmatrix} \mathcal{B}^*(c - y_\rho) \\ z_\rho - x \end{pmatrix} + t \begin{pmatrix} \mathcal{B}^*(c - y_\rho^{(0,0)}) \\ z_\rho^{(0,0)} - x^{(0,0)} \end{pmatrix}. \quad (60)$$

In practical computations, the variable \hat{x} is not formed explicitly. Following Theorem 7, we instead solve the system in (x, s, λ) :

$$\begin{pmatrix} \mathcal{A} & 0 & 0 \\ 0 & \mathcal{I}_E & \mathcal{A}^* \\ \mathcal{H}^{-1}\mathcal{W} & \rho^{-1}\mathcal{H}^{-1} & 0 \end{pmatrix} \begin{pmatrix} \Delta x \\ \Delta s \\ \Delta \lambda \end{pmatrix} = - \begin{pmatrix} \mathcal{A}x - b \\ \mathcal{A}^*\lambda + s - c \\ x - z_\rho \end{pmatrix} + t \begin{pmatrix} 0 \\ \mathcal{A}^*\lambda^{(0,0)} + s^{(0,0)} - c \\ x^{(0,0)} - z_\rho^{(0,0)} \end{pmatrix}. \quad (61)$$

The resulting search direction coincides with the one obtained by solving (60) under the constraint $\mathcal{A}x = b$. This equivalence is formalized in the following corollary.

Corollary 2 *Let (x, s, λ) satisfy the affine constraint $\mathcal{A}x = b$. For the given point $(x^{(0,0)}, s^{(0,0)}, \lambda^{(0,0)})$ and any $\mu^{(0)} > 0$, $\rho > 0$, suppose that $(\Delta x, \Delta s, \Delta \lambda)$ solves (61). Then the pair $(\Delta \hat{x}, \Delta s) := (\mathcal{B}^* \Delta x, \Delta s)$ is the unique solution of (60). Conversely, if $(\Delta \hat{x}, \Delta s)$ solves (60), define*

$$\Delta \lambda := (\mathcal{A}\mathcal{A}^*)^{-1} \mathcal{A}(-s - \Delta s + c - \mathcal{A}^*\lambda + t(\mathcal{A}^*\lambda^{(0,0)} + s^{(0,0)} - c)). \quad (62)$$

Then $(\Delta x, \Delta s, \Delta \lambda) := (\mathcal{B}\Delta \hat{x}, \Delta s, \Delta \lambda)$ is the unique solution of (61).

Proof The proof follows the same arguments as in Theorem 7, with a minor modification due to the shift term. Details are omitted. \square

We are now ready to state the first phase of the proposed method. Starting from an arbitrary point $w^{(0,0)} \in K(\theta_\rho)$, the purpose of this phase is to follow the perturbed minimax problems defined by $\eta_{t,\rho}$ and to drive the iterate into the neighborhood $\mathcal{N}(\kappa, \mu^{(0)}, \rho)$ for the fixed smoothing parameter $\mu^{(0)}$. The parameter t plays the role of a homotopy parameter: for a suitable $t^{(0)} \in (0, 1]$ such that

$$(1 - t^{(0)})\delta_\rho(w^{(0,0)}; \mu^{(0)}) \leq \frac{\kappa}{2}, \quad (63)$$

the initial point is close to the saddle point of the perturbed problem, while decreasing t gradually removes the perturbation and recovers the original reduced minimax problem.

Algorithm 1 The first phase of PFSNM

Require: $w^{(0,0)} \in K(\theta_\rho)$, $\lambda^{(0,0)} \in \mathbb{R}^m$, $\rho > 0$, $\mu^{(0)} > 0$, and $t^{(0)} \in (0, 1]$ satisfying (63).

- 1: **for** $j = 0, 1, 2, \dots$ **do**
- 2: **if** $\delta_\rho(w^{(0,j)}; \mu^{(0)}) \leq \kappa$ **then**
- 3: Compute the Newton direction $\Delta v^{(0,j)}$ from (40).
- 4: **return** $v^{(0)} = v^{(0,j)} + \Delta v^{(0,j)}$.
- 5: **else**
- 6: Update

$$\alpha^{(j)} = \min \left\{ \frac{\kappa}{4t^{(j)} \left\| (D_{ww}^2 \eta_\rho(w^{(0,j)}; \mu^{(0)}))^{-1} \nabla_w \eta_\rho(w^{(0,0)}; \mu^{(0)}) \right\|_{\eta_\rho, w^{(0,j)}}}, 1 \right\}. \quad (64)$$

- 7: Set $t^{(j+1)} = (1 - \alpha^{(j)})t^{(j)}$.
- 8: Compute the search direction $\Delta v^{(0,j)}$ from (61) with $t = t^{(j+1)}$ and set

$$v^{(0,j+1)} = v^{(0,j)} + \Delta v^{(0,j)}.$$

- 9: **end if**
 - 10: **end for**
-

Throughout Algorithm 1, the iterates $(x^{(0,j)}, s^{(0,j)}, \lambda^{(0,j)})$ always satisfy the primal constraint, as follows from (61). When Algorithm 1 terminates, the second equation of (40) yields

$$\mathcal{A}^* \lambda^{(0)} + s^{(0)} - c = 0.$$

Furthermore, since $\delta_\rho(w^{(0,j)}; \mu^{(0)}) \leq \kappa = 0.1 < 1$, Theorem 3(iii) yields

$$\xi_\rho(w^{(0)}; \mu^{(0)}) \leq \left(\frac{\delta_\rho(w^{(0,j)}; \mu^{(0)})}{1 - \delta_\rho(w^{(0,j)}; \mu^{(0)})} \right)^2 \leq \frac{1}{2} \delta_\rho(w^{(0,j)}; \mu^{(0)}) \leq \kappa.$$

Hence $v^{(0)} \in \mathcal{N}(\kappa, \mu^{(0)}, \rho)$.

Once a point in $\mathcal{N}(\kappa, \mu^{(0)}, \rho)$ has been obtained, the second phase decreases the smoothing parameter and recenters the iterate for each new value of μ . The analysis in Section 5 will show that, after each update of μ , only one Newton step is sufficient to return to the neighborhood.

Algorithm 2 The second phase of PFSNM

Require: $v^{(0)} \in \mathcal{N}(\kappa, \mu^{(0)}, \rho)$, $\rho > 0$, $\mu^{(0)} > 0$, $\varepsilon > 0$, and $\sigma \in (0, 1)$.

```

1: for  $k = 0, 1, 2, \dots$  do
2:   if  $\mu^{(k)} \leq \varepsilon$  then
3:     return  $v^{(k)}$ .
4:   else
5:     Update  $\mu^{(k+1)} = \sigma \mu^{(k)}$ .
6:     Compute the search direction  $\Delta v^{(k)}$  from (40) with  $\mu = \mu^{(k+1)}$ , and set

```

$$v^{(k+1)} = v^{(k)} + \Delta v^{(k)}.$$

```

7:   end if
8: end for

```

After each reduction of the smoothing parameter, a single full Newton step is sufficient to recenter the iterate; more precisely, the resulting point $v^{(k+1)}$ belongs to the new neighborhood $\mathcal{N}(\kappa, \mu^{(k+1)}, \rho)$. This fact is established in Theorem 12. Therefore, Algorithm 2 retains the standard path-following structure.

Several remarks on Algorithms 1 and 2 are in order:

- (i) In practical computations, the variable \hat{x} is never formed explicitly. Computations are performed directly with the primal variable x since $\delta_\rho(w^{(0,j)}; \mu^{(0)})$ can be evaluated from (x, s, λ) ; see Remark 3 for details.
- (ii) There is no need to form the Newton systems of η_ρ or $\eta_{t,\rho}$ with respect to (\hat{x}, s) explicitly. By Theorem 7 and Corollary 2, updating (x, s, λ) is in fact equivalent to updating (\hat{x}, s) .
- (iii) The iterate entering Algorithm 2 satisfies the primal and dual constraints. Consequently, by (40) and the iteration scheme, all subsequent iterates remain feasible:

$$\mathcal{A}x^{(k)} = b, \quad \mathcal{A}^* \lambda^{(k)} + s^{(k)} = c, \quad \forall k \geq 0. \quad (65)$$

- (iv) Once Algorithm 2 terminates, we have

$$\mu^{(k)} \leq \varepsilon \quad \text{and} \quad \xi_\rho(w^{(k)}; \mu^{(k)}) = \|\nabla_w \eta_\rho(w^{(k)}; \mu^{(k)})\|_{\eta_\rho, w^{(k)}, \mu^{(k)}}^* \leq \kappa.$$

It follows from the definition of ξ_ρ and Corollary 1 that

$$\begin{aligned} \|z_\rho^{(k)} - x^{(k)}\| &\leq \sqrt{\langle z_\rho^{(k)} - x^{(k)}, \mathcal{H}(z_\rho^{(k)} - x^{(k)}) \rangle} \\ &\leq \sqrt{\frac{\mu^{(k)}}{\rho}} \|\nabla_w \eta_\rho(w^{(k)}; \mu^{(k)})\|_{\eta_\rho, w^{(k)}, \mu^{(k)}}^* \\ &\leq \sqrt{\frac{\varepsilon}{\rho}} \kappa. \end{aligned}$$

Recall that $\Phi_\rho(x^{(k)}, s^{(k)}; \mu^{(k)}) = 2(x^{(k)} - z_\rho(x^{(k)}, s^{(k)}; \mu^{(k)}))$. By (iii) and (iv), when Algorithm 2 terminates, an approximate KKT triple $(x^{(k)}, s^{(k)}, \lambda^{(k)})$ for the original SCP problem (1) is obtained, satisfying

$$\mathcal{A}x^{(k)} = b, \mathcal{A}^* \lambda^{(k)} + s^{(k)} = c, \|\Phi_\rho(x^{(k)}, s^{(k)}; \mu^{(k)})\| \leq 2\kappa \sqrt{\frac{\varepsilon}{\rho}}. \quad (66)$$

4.3 Linear systems in the algorithms

In practical computations, the primal constraint is satisfied at all iterates. Thus, the Newton systems (61) and (40) arising in Algorithms 1 and 2 can be written in the unified form

$$\begin{pmatrix} \mathcal{A} & 0 & 0 \\ 0 & \mathcal{I}_{\mathbb{E}} & \mathcal{A}^* \\ \mathcal{H}^{-1} \mathcal{W} & \rho^{-1} \mathcal{H}^{-1} & 0 \end{pmatrix} \begin{pmatrix} \Delta x \\ \Delta s \\ \Delta \lambda \end{pmatrix} = \begin{pmatrix} 0 \\ r_1 \\ r_2 \end{pmatrix}, \quad (67)$$

where

$$\begin{aligned} r_1 &= \begin{cases} -\mathcal{A}^* \lambda - s + c + t(\mathcal{A}^* \lambda^{(0,0)} + s^{(0,0)} - c), & \text{for the first phase system (61);} \\ 0, & \text{for the second phase system (40),} \end{cases} \\ r_2 &= \begin{cases} z_\rho - x - t(z_\rho^{(0,0)} - x^{(0,0)}), & \text{for the first phase system (61);} \\ z_\rho - x, & \text{for the second phase system (40).} \end{cases} \end{aligned}$$

Directly solving the full Newton system (67) is computationally expensive, particularly for large-scale problems when the dimensions of the cone variables x and s are significantly larger than the number of constraints. To reduce the computational cost, we eliminate Δx and Δs from (67), which leads to the following Schur-complement system:

$$\mathcal{A} \mathcal{W}^{-1} \mathcal{A}^* \Delta \lambda = \mathcal{A} \mathcal{W}^{-1} r_1 - \rho \mathcal{A} \mathcal{W}^{-1} \mathcal{H} r_2, \quad (68a)$$

$$\Delta s = r_1 - \mathcal{A}^* \Delta \lambda, \quad (68b)$$

$$\Delta x = \mathcal{W}^{-1} (\mathcal{H} r_2 - \rho^{-1} \Delta s). \quad (68c)$$

For both IPMs and classical SNMs, the dominant computational cost typically comes from forming and factorizing the Schur complement $\mathcal{A} \mathcal{D} \mathcal{A}^*$. In our method, $\mathcal{D} = \mathcal{W}^{-1}$, where \mathcal{W} is an iterate-dependent operator determined by the barrier function in PFSNM. Accordingly, improving the efficiency of forming $\mathcal{A} \mathcal{D} \mathcal{A}^*$ is crucial for large-scale computation. To this end, Proposition 3 provides closed-form expressions for $\mathcal{A} \mathcal{D} \mathcal{A}^*$ in PFSNM for the three most common symmetric cones.

Proposition 3 *Let \mathbb{K} be one of the symmetric cones considered below, and let e denote the corresponding Jordan identity element. Then the corresponding Schur complement admits the following explicit representations.*

(i) *Let $\mathbb{K} = \mathbb{R}_+^n$. Then, for any $z \in \mathbb{R}_{++}^n$, $\phi(z) = -\sum_{i=1}^n \ln z_i$, and*

$$\mathcal{A}W^{-1}\mathcal{A}^* = \frac{\rho}{\mu} \mathcal{A}(\text{Diag}(z_\rho))^2 \mathcal{A}^*.$$

(ii) *Let $\mathbb{K} = \mathbb{Q}^{n+1}$. Then, for any $z \in \text{int}(\mathbb{Q}^{n+1})$, $\phi(z) = -\ln(z_0^2 - \|\bar{z}\|^2)$, and*

$$\mathcal{A}W^{-1}\mathcal{A}^* = \frac{\rho}{\mu} \left(\det(z_\rho) \mathcal{A}\mathcal{A}^* + 2(\mathcal{A}z_\rho)(\mathcal{A}z_\rho)^* - 2\det(z_\rho)(\mathcal{A}e)(\mathcal{A}e)^* \right).$$

(iii) *Let $\mathbb{K} = \mathbb{S}_+^n$. Then, for any $Z \in \mathbb{S}_{++}^n$, $\phi(Z) = -\ln \det(Z)$, and*

$$\mathcal{A}W^{-1}\mathcal{A}^* = \frac{\rho}{\mu} \mathcal{A}(Z_\rho \otimes_s Z_\rho) \mathcal{A}^*.$$

Proof By definition, $W = \frac{\mu}{\rho} D^2 \phi(z_\rho)$. The results follow directly from the explicit formulas (see [44, Proposition 2.6.1]) for $D^2 \phi$. \square

The importance of explicit Schur-complement formulas has already been noted in the SDP literature. The SNM in [8], based on the smoothing FB function, has a Schur-complement formation cost comparable to that of the most expensive Alizadeh–Haerberly–Overton (AHO) direction in IPMs. If the smoothing CHKS function is used instead, the formation cost becomes lower than that of AHO, but remains higher than that of the Nesterov–Todd (NT) direction. In our earlier work [48], we showed that once an explicit formula for the Schur complement is available, the formation cost can be reduced to the same order as that of the NT direction. Compared with [48], this paper leverages self-concordant properties to derive this explicit Schur-complement formula in a simpler and more direct way.

For SOCP, the advantage of the explicit Schur complement is even more significant. As shown in case (ii) of Proposition 3, the Schur complement takes the form of a scaled matrix plus two rank-one updates. However, the vector $u := \mathcal{A}z_\rho$ appearing in these rank-one terms is typically dense, which causes the resulting Schur complement to be dense as well. Figure 2 illustrates this structure and shows how these components combine to yield a fully dense matrix. This density poses a major computational challenge in large-scale settings. Even accelerating the evaluation of \mathcal{D} as described in [15] does not solve the problem, because the Schur complement remains dense. The explicit representation in Proposition 3 avoids forming this dense matrix. The terms $\mathcal{A}\mathcal{A}^*$ and $\mathcal{A}e$ depend only on the problem data and can be precomputed once. Each subsequent iteration then requires only one matrix-vector product $u = \mathcal{A}z_\rho$, along with simple low-rank updates and the scalar $\det(z_\rho)$. With this structure, one can apply either the product-form Cholesky factorization approach in [1] or the expanded sparse representation technique in [49]. Both approaches exploit the low-rank structure and avoid forming a dense Schur complement.

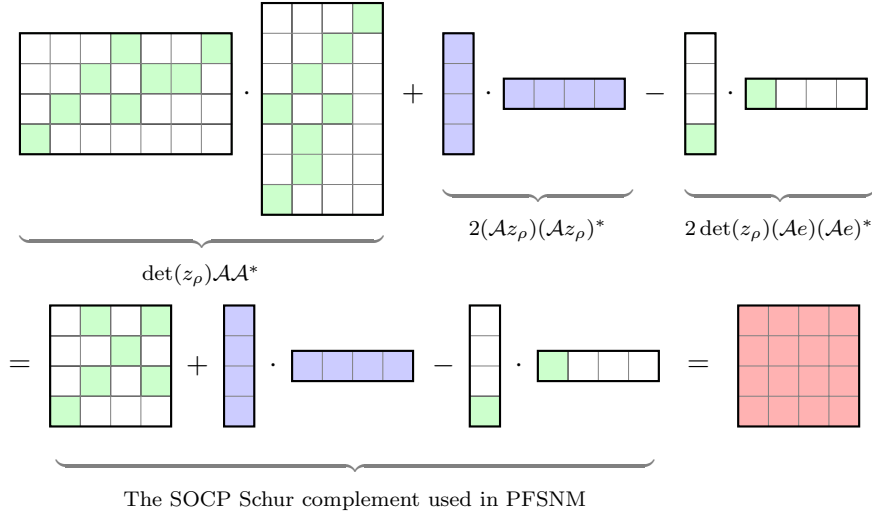


Fig. 2: Structure of the SOCP Schur complement in PFSNM

5 Complexity analysis

In this section, we establish a polynomial iteration complexity for PFSNM applied to SCP. The analysis consists of two parts. We first derive an iteration complexity for the first phase. Starting from the point produced by this phase, Algorithm 2 then attains an iteration complexity of order $\mathcal{O}(\sqrt{\nu} \ln(1/\varepsilon))$, matching the classical short-step interior-point complexity [43].

The iteration complexity for the first phase is presented in the following theorem.

Theorem 8 *Suppose that $w^{(0,0)} \in K(\theta_\rho)$ and that $t^{(0)}$ in Algorithm 1 satisfies (63). Then Algorithm 1 requires at most*

$$\mathcal{O}\left(1 + \frac{4t^{(0)}}{\kappa} \Theta_1\left(\frac{\theta_\rho(w^{(0,0)}; \mu^{(0)})}{\mu^{(0)}}\right)\right) \quad (69)$$

iterations to obtain a starting point $v^{(0)} \in \mathcal{N}(\kappa, \mu^{(0)}, \rho)$, where $\Theta_1(\cdot)$ is a properly chosen universal positive, continuous, and nondecreasing function on \mathbb{R}_+ .

Proof Since μ remains fixed in the first phase, we write $\eta_\rho(w)$ and $\eta_{t,\rho}(w)$ in place of $\eta_\rho(w; \mu^{(0)})$ and $\eta_{t,\rho}(w; \mu^{(0)})$, respectively. Define the merit function associated with $\eta_{t,\rho}$ by

$$\delta_{t,\rho}(w) := \|(D_{ww}^2 \eta_\rho(w))^{-1} \nabla_w \eta_{t,\rho}(w)\|_{\eta_{t,\rho}, w} = \|(D_{ww}^2 \eta_\rho(w))^{-1} \nabla_w \eta_{t,\rho}(w)\|_{\eta_\rho, w}.$$

Noting that $\nabla_w \eta_{t,\rho}(w) = \nabla_w \eta_\rho(w) - t \nabla_w \eta_\rho(w^{(0,0)})$,

$$\delta_{t^{(0)}, \rho}(w^{(0,0)}) = (1 - t^{(0)}) \delta_\rho(w^{(0,0)}). \quad (70)$$

We now prove by induction that $\delta_{t^{(j)},\rho}(w^{(0,j)}) \leq \frac{\kappa}{2}$ at each iteration j . For $j = 0$, the claim follows from (63) and (70). Assume that $\delta_{t^{(j)},\rho}(w^{(0,j)}) \leq \frac{\kappa}{2}$ at the j -th iteration. Then

$$\begin{aligned} & \delta_{t^{(j+1)},\rho}(w^{(0,j)}) - \delta_{t^{(j)},\rho}(w^{(0,j)}) \\ &= \|(D_{ww}^2 \eta_\rho(w^{(0,j)}))^{-1} \nabla_w \eta_{t^{(j+1)},\rho}(w^{(0,j)})\|_{\eta_\rho, w^{(0,j)}} \\ & \quad - \|(D_{ww}^2 \eta_\rho(w^{(0,j)}))^{-1} \nabla_w \eta_{t^{(j)},\rho}(w^{(0,j)})\|_{\eta_\rho, w^{(0,j)}} \\ & \leq \alpha^{(j)} t^{(j)} \|(D_{ww}^2 \eta_\rho(w^{(0,j)}))^{-1} \nabla_w \eta_\rho(w^{(0,0)})\|_{\eta_\rho, w^{(0,j)}} \\ & \leq \frac{\kappa}{4}. \end{aligned}$$

Here the first inequality follows from the identity for $\nabla_w \eta_{t,\rho}(w)$ and from the fact that $\|\cdot\|_{\eta_\rho, w^{(0,j)}}$ defines a norm. The second inequality follows from (64). Thus,

$$\delta_{t^{(j+1)},\rho}(w^{(0,j)}) \leq \frac{\kappa}{2} + \frac{\kappa}{4} = \frac{3\kappa}{4} < \kappa. \quad (71)$$

By (71) and Theorem 3(ii)–(iii), we have

$$\delta_{t^{(j+1)},\rho}(w^{(0,j+1)}) \leq \left(\frac{\delta_{t^{(j+1)},\rho}(w^{(0,j)})}{1 - \delta_{t^{(j+1)},\rho}(w^{(0,j)})} \right)^2 \leq \frac{\kappa}{2},$$

which completes the induction argument. Hence,

$$\delta_{t^{(j)},\rho}(w^{(0,j)}) \leq \frac{\kappa}{2}, \quad \forall j \geq 0. \quad (72)$$

By applying Nemirovski's estimate [31, Lemma 8.3(a)] to the standard self-concordant convex-concave function $\frac{\eta_\rho(w; \mu^{(0)})}{\mu^{(0)}}$, there exists a universal positive, continuous, and nondecreasing function Θ_1 such that

$$\|(D_{ww}^2 \eta_\rho(w^{(0,j)}))^{-1} \nabla_w \eta_\rho(w^{(0,0)})\|_{\eta_\rho, w^{(0,j)}} \leq \Theta_1 \left(\frac{\theta_\rho(w^{(0,0)}; \mu^{(0)})}{\mu^{(0)}} \right). \quad (73)$$

It remains to estimate the number of updates of t . If $\alpha^{(j)} = 1$, then $t^{(j+1)} = (1 - \alpha^{(j)})t^{(j)} = 0$. Hence, by (72),

$$\delta_\rho(w^{(0,j+1)}; \mu^{(0)}) = \delta_{t^{(j+1)},\rho}(w^{(0,j+1)}) \leq \frac{\kappa}{2}.$$

Thus Algorithm 1 terminates after at most one additional Newton step.

We next consider the case where $\alpha^{(j)} < 1$. Using the definition of $\alpha^{(j)}$ in (64), we have

$$\alpha^{(j)} t^{(j)} = \frac{\kappa}{4 \|(D_{ww}^2 \eta_\rho(w^{(0,j)}; \mu^{(0)}))^{-1} \nabla_w \eta_\rho(w^{(0,0)}; \mu^{(0)})\|_{\eta_\rho, w^{(0,j)}}}.$$

Therefore,

$$\begin{aligned} t^{(j+1)} &= (1 - \alpha^{(j)})t^{(j)} \\ &= t^{(j)} - \frac{\kappa}{4 \|(D_{ww}^2 \eta_\rho(w^{(0,j)}; \mu^{(0)}))^{-1} \nabla_w \eta_\rho(w^{(0,0)}; \mu^{(0)})\|_{\eta_\rho, w^{(0,j)}}}. \end{aligned}$$

By (73), this implies

$$t^{(j+1)} \leq t^{(j)} - \frac{\kappa}{4\Theta_1 \left(\frac{\theta_\rho(w^{(0,0)}; \mu^{(0)})}{\mu^{(0)}} \right)}.$$

Consequently, as long as Algorithm 1 has not yet reached a point satisfying

$$t^{(j)} \Theta_1 \left(\frac{\theta_\rho(w^{(0,0)}; \mu^{(0)})}{\mu^{(0)}} \right) \leq \frac{\kappa}{2},$$

the parameter $t^{(j)}$ decreases by at least $\frac{\kappa}{4\Theta_1 \left(\frac{\theta_\rho(w^{(0,0)}; \mu^{(0)})}{\mu^{(0)}} \right)}$ at each update. Hence,

after at most

$$\mathcal{O} \left(\frac{4t^{(0)}}{\kappa} \Theta_1 \left(\frac{\theta_\rho(w^{(0,0)}; \mu^{(0)})}{\mu^{(0)}} \right) \right)$$

updates, we obtain an index j such that $t^{(j)} \Theta_1 \left(\frac{\theta_\rho(w^{(0,0)}; \mu^{(0)})}{\mu^{(0)}} \right) \leq \frac{\kappa}{2}$. Combining this estimate with (72) and (73), we get

$$\begin{aligned} \delta_\rho(w^{(0,j)}; \mu^{(0)}) &= \left\| (D_{ww}^2 \eta_\rho(w^{(0,j)}))^{-1} \nabla_w \eta_\rho(w^{(0,j)}) \right\|_{\eta_\rho, w^{(0,j)}} \\ &\leq \delta_{t^{(j)}, \rho}(w^{(0,j)}) + t^{(j)} \left\| (D_{ww}^2 \eta_\rho(w^{(0,j)}))^{-1} \nabla_w \eta_\rho(w^{(0,0)}) \right\|_{\eta_\rho, w^{(0,j)}} \\ &\leq \frac{\kappa}{2} + t^{(j)} \Theta_1 \left(\frac{\theta_\rho(w^{(0,0)}; \mu^{(0)})}{\mu^{(0)}} \right) \leq \kappa. \end{aligned}$$

Therefore, Algorithm 1 terminates. The final Newton step computed from (40) then gives a point $v^{(0)} \in \mathcal{N}(\kappa, \mu^{(0)}, \rho)$. Thus Algorithm 1 requires at most

$$\mathcal{O} \left(1 + \frac{4t^{(0)}}{\kappa} \Theta_1 \left(\frac{\theta_\rho(w^{(0,0)}; \mu^{(0)})}{\mu^{(0)}} \right) \right)$$

iterations to obtain a starting point $v^{(0)} \in \mathcal{N}(\kappa, \mu^{(0)}, \rho)$. \square

Having established the iteration complexity for the first phase of PFSNM, we now turn to analyze the iteration complexity of Algorithm 2. As a preliminary step, Theorems 9 and 10 quantify the effect of updating the smoothing parameter μ on both $\nabla_w \eta_\rho(w; \mu)$ and $S_{\eta_\rho}(w; \mu)$. For notational simplicity, we omit the arguments $(w; \mu)$ and write, for example, $\nabla_w \eta_\rho := \nabla_w \eta_\rho(w; \mu)$ whenever first- or second-order derivatives of η_ρ with respect to $w = (\hat{x}, s)$ are mentioned. All derivatives with respect to μ are denoted by prime.

Theorem 9 For any $\mu > 0$, $\rho > 0$, any direction $h = (h_{\hat{x}}, h_s) \in \hat{\mathbb{E}} \times \mathbb{E}$, and any point $w = (\hat{x}, s) \in \hat{\mathbb{E}} \times \mathbb{E}$,

$$|\langle h, \nabla_w \eta'_\rho(w; \mu) \rangle| \leq \sqrt{\frac{2\nu}{\mu}} \sqrt{S_{\eta_\rho}(w; \mu)[h, h]}. \quad (74)$$

Proof Combining Theorem 4 and Corollary 1 yields

$$\nabla_w \eta'_\rho(w; \mu) = \begin{pmatrix} -\mathcal{B}^* y'_\rho \\ z'_\rho \end{pmatrix} = \begin{pmatrix} \mathcal{B}^* \mathcal{H}^{-1} \nabla \phi(z_\rho) \\ -\rho^{-1} \mathcal{H}^{-1} \nabla \phi(z_\rho) \end{pmatrix}.$$

For any $h = (h_{\hat{x}}, h_s) \in \hat{\mathbb{E}} \times \mathbb{E}$,

$$\langle \nabla_w \eta'_\rho(w; \mu), h \rangle = \langle \mathcal{B} h_{\hat{x}}, \mathcal{H}^{-1} \nabla \phi(z_\rho) \rangle - \rho^{-1} \langle h_s, \mathcal{H}^{-1} \nabla \phi(z_\rho) \rangle.$$

Let $h_x = \mathcal{B} h_{\hat{x}}$. Then,

$$\begin{aligned} |\langle \nabla_w \eta'_\rho, h \rangle| &\leq \left| \langle h_x, \mathcal{H}^{-1} \nabla \phi(z_\rho) \rangle \right| + \rho^{-1} \left| \langle h_s, \mathcal{H}^{-1} \nabla \phi(z_\rho) \rangle \right| \\ &= \left| \langle h_x, \mathcal{H}^{-\frac{1}{2}} \mathcal{W}^{\frac{1}{2}} \mathcal{W}^{-\frac{1}{2}} \mathcal{H}^{-\frac{1}{2}} \nabla \phi(z_\rho) \rangle \right| + \rho^{-1} \left| \langle h_s, \mathcal{H}^{-\frac{1}{2}} \mathcal{H}^{-\frac{1}{2}} \nabla \phi(z_\rho) \rangle \right| \\ &\leq \sqrt{\langle h_x, \mathcal{H}^{-1} \mathcal{W} h_x \rangle} \sqrt{\langle \nabla \phi(z_\rho), \mathcal{W}^{-1} \mathcal{H}^{-1} \nabla \phi(z_\rho) \rangle} \\ &\quad + \rho^{-1} \sqrt{\langle h_s, \mathcal{H}^{-1} h_s \rangle} \sqrt{\langle \nabla \phi(z_\rho), \mathcal{H}^{-1} \nabla \phi(z_\rho) \rangle}. \end{aligned} \tag{75}$$

Since $\mathcal{H}^{-1} = (\mathcal{I}_{\mathbb{E}} + \mathcal{W})^{-1}$, we have

$$\mathcal{W}^{-1} \mathcal{H}^{-1} \prec \mathcal{W}^{-1}, \quad \mathcal{H}^{-1} \prec \mathcal{W}^{-1},$$

which together with $\mathcal{W} = \frac{\mu}{\rho} D^2 \phi(z_\rho)$ and (10) implies

$$\begin{aligned} \sqrt{\langle \nabla \phi(z_\rho), \mathcal{W}^{-1} \mathcal{H}^{-1} \nabla \phi(z_\rho) \rangle} &\leq \sqrt{\frac{\rho}{\mu} \langle \nabla \phi(z_\rho), (D^2 \phi(z_\rho))^{-1} \nabla \phi(z_\rho) \rangle} = \sqrt{\frac{\rho \nu}{\mu}}, \\ \sqrt{\langle \nabla \phi(z_\rho), \mathcal{H}^{-1} \nabla \phi(z_\rho) \rangle} &\leq \sqrt{\frac{\rho}{\mu} \langle \nabla \phi(z_\rho), (D^2 \phi(z_\rho))^{-1} \nabla \phi(z_\rho) \rangle} = \sqrt{\frac{\rho \nu}{\mu}}. \end{aligned} \tag{76}$$

Combining (75), (76) and Corollary 1 yields

$$\begin{aligned} |\langle \nabla_w \eta'_\rho, h \rangle| &\leq \sqrt{\frac{\nu}{\mu}} \left(\sqrt{\langle h_{\hat{x}}, D_{\hat{x}\hat{x}}^2 \eta_\rho h_{\hat{x}} \rangle} + \sqrt{-\langle h_s, D_{ss}^2 \eta_\rho h_s \rangle} \right) \\ &\leq \sqrt{\frac{2\nu}{\mu}} \sqrt{S_{\eta_\rho}[h, h]}. \end{aligned}$$

This completes the proof. \square

Theorem 10 For any $\mu > 0$, $\rho > 0$, any direction $h = (h_{\hat{x}}, h_s) \in \hat{\mathbb{E}} \times \mathbb{E}$, and any point $w = (\hat{x}, s) \in \hat{\mathbb{E}} \times \mathbb{E}$,

$$|S'_{\eta_\rho}(w; \mu)[h, h]| \leq \frac{1 + 2\sqrt{\nu}}{\mu} S_{\eta_\rho}(w; \mu)[h, h]. \tag{77}$$

Proof Let $h_x = \mathcal{B} h_{\hat{x}}$ and $\bar{h} = (\bar{h}_x, \bar{h}_s) = (\mathcal{H}^{-1} h_x, \mathcal{H}^{-1} h_s)$. Define

$$\omega(\mu) := S_{\eta_\rho}(w; \mu)[h, h].$$

By Corollary 1,

$$\omega(\mu) = \omega_x(\mu) + \omega_s(\mu),$$

where $\omega_x(\mu) := \rho \langle h_x, (\mathcal{I}_{\mathbb{E}} - \mathcal{H}^{-1})h_x \rangle$, $\omega_s(\mu) := \rho^{-1} \langle h_s, \mathcal{H}^{-1}h_s \rangle$. Differentiating $\omega_x(\mu)$ with respect to μ yields

$$\begin{aligned} |\omega'_x(\mu)| &= \left| \langle \mathcal{H}^{-1}h_x, D^2\phi(z_\rho)\mathcal{H}^{-1}h_x \rangle + \mu D^3\phi(z_\rho)[z'_\rho, \mathcal{H}^{-1}h_x, \mathcal{H}^{-1}h_x] \right| \\ &\leq \left| \frac{\rho}{\mu} \langle h_x, \mathcal{H}^{-1}\mathcal{W}\mathcal{H}^{-1}h_x \rangle \right| + \left| \mu D^3\phi(z_\rho)[z'_\rho, \bar{h}_x, \bar{h}_x] \right|. \end{aligned} \quad (78)$$

By Corollary 1 and the inequality $\mathcal{H}^{-1}\mathcal{W}\mathcal{H}^{-1} \prec \mathcal{H}^{-1}\mathcal{W}$, we have

$$\left| \rho \langle h_x, \mathcal{H}^{-1}\mathcal{W}\mathcal{H}^{-1}h_x \rangle \right| \leq D_{\hat{x}\hat{x}}^2\eta_\rho[h_{\hat{x}}, h_{\hat{x}}]. \quad (79)$$

Since ϕ is a standard self-concordant convex function, it follows from [33, Proposition 9.1.1] and (79) that

$$\begin{aligned} \left| \mu D^3\phi(z_\rho)[z'_\rho, \bar{h}_x, \bar{h}_x] \right| &\leq 2\mu \sqrt{D^2\phi(z_\rho)[z'_\rho, z'_\rho] D^2\phi(z_\rho)[\bar{h}_x, \bar{h}_x]} \\ &= 2\rho \sqrt{D^2\phi(z_\rho)[z'_\rho, z'_\rho]} \langle h_x, \mathcal{H}^{-1}\mathcal{W}\mathcal{H}^{-1}h_x \rangle \\ &\leq 2\sqrt{D^2\phi(z_\rho)[z'_\rho, z'_\rho]} D_{\hat{x}\hat{x}}^2\eta_\rho[h_{\hat{x}}, h_{\hat{x}}]. \end{aligned} \quad (80)$$

By Theorem 4 and the inequality $\mathcal{H}^{-1} \prec \mathcal{W}^{-1}$, we have

$$\begin{aligned} \sqrt{D^2\phi(z_\rho)[z'_\rho, z'_\rho]} &= \frac{1}{\rho} \sqrt{\langle \nabla\phi(z_\rho), \mathcal{H}^{-1}D^2\phi(z_\rho)\mathcal{H}^{-1}\nabla\phi(z_\rho) \rangle} \\ &\leq \frac{1}{\rho} \sqrt{\langle \nabla\phi(z_\rho), \mathcal{W}^{-1}D^2\phi(z_\rho)\mathcal{W}^{-1}\nabla\phi(z_\rho) \rangle} \\ &= \frac{1}{\mu} \sqrt{\langle \nabla\phi(z_\rho), (D^2\phi(z_\rho))^{-1}\nabla\phi(z_\rho) \rangle} \\ &= \frac{\sqrt{\nu}}{\mu}. \end{aligned} \quad (81)$$

Combining (78)–(81) yields

$$|\omega'_x(\mu)| \leq \frac{1+2\sqrt{\nu}}{\mu} D_{\hat{x}\hat{x}}^2\eta_\rho[h_{\hat{x}}, h_{\hat{x}}]. \quad (82)$$

Similarly, we obtain

$$|\omega'_s(\mu)| \leq \frac{1+2\sqrt{\nu}}{\mu} \left(-D_{ss}^2\eta_\rho[h_s, h_s] \right). \quad (83)$$

Since $\omega(\mu) = \omega_x(\mu) + \omega_s(\mu)$, it follows from the triangle inequality, (82), and (83) that

$$\begin{aligned} |\omega'(\mu)| &\leq \frac{1+2\sqrt{\nu}}{\mu} D_{\hat{x}\hat{x}}^2\eta_\rho[h_{\hat{x}}, h_{\hat{x}}] - \frac{1+2\sqrt{\nu}}{\mu} D_{ss}^2\eta_\rho[h_s, h_s] \\ &= \frac{1+2\sqrt{\nu}}{\mu} S_{\eta_\rho}[h, h]. \end{aligned}$$

This completes the proof. \square

The preceding two theorems quantify how the first- and second-order quantities induced by the reduced BAL function vary when the smoothing parameter is

changed. These estimates will be used to control the effect of the parameter μ update in the path-following phase. Before deriving the final complexity bound, we also need an estimate that connects the computable quantity $\xi_\rho(w; \mu)$ with the primal-dual gap $\theta_\rho(w; \mu)$. For this purpose, we introduce auxiliary displacement measures from the current point to the exact partial minimizer and maximizer of the reduced minimax problem:

$$\tilde{\delta}_{\hat{x}, \rho}(w; \mu) = \sqrt{\frac{1}{\mu} \langle \widetilde{\Delta \hat{x}}, D_{\hat{x}\hat{x}}^2 \eta_\rho(w; \mu) \widetilde{\Delta \hat{x}} \rangle}, \quad (84a)$$

$$\tilde{\delta}_{s, \rho}(w; \mu) = \sqrt{-\frac{1}{\mu} \langle \widetilde{\Delta s}, D_{ss}^2 \eta_\rho(w; \mu) \widetilde{\Delta s} \rangle}, \quad (84b)$$

$$\tilde{\delta}_\rho(w; \mu) = \sqrt{(\tilde{\delta}_{\hat{x}, \rho}(w; \mu))^2 + (\tilde{\delta}_{s, \rho}(w; \mu))^2} = \|\widetilde{\Delta w}\|_{\eta_\rho, w}, \quad (84c)$$

where $\widetilde{\Delta \hat{x}} = \hat{x} - \hat{x}_\rho(s, \mu)$, $\widetilde{\Delta s} = s - s_\rho(\hat{x}, \mu)$, and $\widetilde{\Delta w} = (\widetilde{\Delta \hat{x}}, \widetilde{\Delta s})$. These quantities are used only in the analysis and are not required in the implementation of the algorithm.

Theorem 11 *For any $\mu > 0$, $\rho > 0$, and any point $w = (\hat{x}, s) \in \hat{\mathbb{E}} \times \mathbb{E}$, suppose that $\kappa = 0.1$ and*

$$\xi_\rho(w; \mu) \leq \kappa.$$

Then the primal-dual gap function satisfies

$$\theta_\rho(w; \mu) \leq \kappa \mu.$$

Proof To quantify the gaps between the current value η_ρ and the primal optimal value, define

$$\begin{aligned} \theta_{\hat{x}, \rho}(\mu) &:= \eta_\rho(\hat{x}, s; \mu) - \eta_\rho(\hat{x}_\rho(s, \mu), s; \mu), \\ \theta_{s, \rho}(\mu) &:= \eta_\rho(\hat{x}, s_\rho(\hat{x}, \mu); \mu) - \eta_\rho(\hat{x}, s; \mu). \end{aligned}$$

If $\xi_\rho(w; \mu) \leq \kappa$, then by Theorem 3(iv),

$$\max \left\{ \tilde{\delta}_{\hat{x}, \rho}(w; \mu), \tilde{\delta}_{s, \rho}(w; \mu) \right\} \leq 2\kappa.$$

Consequently, we have

$$\begin{aligned} \theta_{s, \rho}(\mu) &= \eta_\rho(\hat{x}, s(\hat{x}, \mu); \mu) - \eta_\rho(\hat{x}, s; \mu) \\ &= - \int_0^1 \langle \widetilde{\Delta s}, \nabla_s \eta_\rho(\hat{x}, s_\rho(\hat{x}, \mu) + \tau \widetilde{\Delta s}; \mu) \rangle d\tau \\ &= - \int_0^1 \int_0^\tau \langle \widetilde{\Delta s}, D_{ss}^2 \eta_\rho(\hat{x}, s_\rho(\hat{x}, \mu) + t \widetilde{\Delta s}; \mu) \widetilde{\Delta s} \rangle dt d\tau \\ &\leq \int_0^1 \int_0^\tau \frac{\mu \tilde{\delta}_{s, \rho}^2}{(1 - \tilde{\delta}_{s, \rho} + t \tilde{\delta}_{s, \rho})^2} dt d\tau \\ &= \left(\frac{\tilde{\delta}_{s, \rho}}{1 - \tilde{\delta}_{s, \rho}} + \ln(1 - \tilde{\delta}_{s, \rho}) \right) \mu \\ &\leq \frac{\kappa}{2} \mu, \end{aligned}$$

where the first inequality follows from Theorem 2 and Proposition 1. By the same argument, we conclude that $\theta_{\hat{x},\rho}(\mu) \leq \frac{\kappa}{2}\mu$. Therefore,

$$\theta_\rho(w; \mu) = \theta_{s,\rho}(\mu) + \theta_{\hat{x},\rho}(\mu) \leq \kappa\mu.$$

This completes the proof. \square

Remark 4 By (54) and Theorem 11, if $\xi_\rho(w; \mu) \leq \kappa$, then

$$|\eta_\rho(w; \mu) - \text{val}(P_\mu)| \leq \kappa\mu.$$

Therefore, the PFSNM can be viewed as a relaxation of the IPM. The interpolation between the subproblem objectives of the two methods is controlled by the parameter μ .

The following lemma relates the merit function $\xi_\rho(w; \mu)$ to the quantities $\nabla_w \eta_\rho(w; \mu)$ and $S_{\eta_\rho}(w; \mu)$, which is crucial for the subsequent complexity analysis.

Lemma 3 For any $\mu > 0$, $\rho > 0$, and any point $w = (\hat{x}, s) \in \hat{\mathbb{E}} \times \mathbb{E}$,

$$\xi_\rho(w; \mu) = \max_{0 \neq h \in \hat{\mathbb{E}} \times \mathbb{E}} \frac{|\langle \nabla_w \eta_\rho(w; \mu), h \rangle|}{\sqrt{\mu S_{\eta_\rho}(w; \mu)[h, h]}}. \quad (85)$$

Proof By Theorem 5, $\eta_\rho(\cdot, s; \mu)$ is nondegenerate μ -self-concordant on $\hat{\mathbb{E}}$ for every $s \in \mathbb{E}$, and $-\eta_\rho(\hat{x}, \cdot; \mu)$ is nondegenerate μ -self-concordant on \mathbb{E} for every $\hat{x} \in \hat{\mathbb{E}}$. It follows from [33, Proposition 2.2.1] that for any nonzero direction $h = (h_{\hat{x}}, h_s) \in \hat{\mathbb{E}} \times \mathbb{E}$,

$$\begin{aligned} \sqrt{\mu} \xi_{\hat{x},\rho}(w; \mu) &\geq \frac{|\langle \nabla_{\hat{x}} \eta_\rho(w; \mu), h_{\hat{x}} \rangle|}{\sqrt{\langle h_{\hat{x}}, D_{\hat{x}\hat{x}}^2 \eta_\rho(w; \mu) h_{\hat{x}} \rangle}}, \\ \sqrt{\mu} \xi_{s,\rho}(w; \mu) &\geq \frac{|\langle \nabla_s \eta_\rho(w; \mu), h_s \rangle|}{\sqrt{-\langle h_s, D_{ss}^2 \eta_\rho(w; \mu) h_s \rangle}}. \end{aligned}$$

Consequently, we have

$$\begin{aligned} &\sqrt{\mu} \xi_\rho \sqrt{\langle h_{\hat{x}}, D_{\hat{x}\hat{x}}^2 \eta_\rho h_{\hat{x}} \rangle - \langle h_s, D_{ss}^2 \eta_\rho h_s \rangle} \\ &= \sqrt{\mu} \sqrt{\xi_{\hat{x},\rho}^2 + \xi_{s,\rho}^2} \sqrt{\langle h_{\hat{x}}, D_{\hat{x}\hat{x}}^2 \eta_\rho h_{\hat{x}} \rangle - \langle h_s, D_{ss}^2 \eta_\rho h_s \rangle} \\ &\geq \sqrt{\mu} \left(\xi_{\hat{x},\rho} \sqrt{\langle h_{\hat{x}}, D_{\hat{x}\hat{x}}^2 \eta_\rho h_{\hat{x}} \rangle} + \xi_{s,\rho} \sqrt{-\langle h_s, D_{ss}^2 \eta_\rho h_s \rangle} \right) \\ &\geq |\langle \nabla_{\hat{x}} \eta_\rho, h_{\hat{x}} \rangle| + |\langle \nabla_s \eta_\rho, h_s \rangle| \\ &\geq |\langle \nabla_w \eta_\rho, h \rangle|, \end{aligned}$$

where the first inequality follows from the Cauchy–Schwarz inequality. Thus,

$$\xi_\rho(w; \mu) \geq \frac{|\langle \nabla_w \eta_\rho(w; \mu), h \rangle|}{\sqrt{\mu S_{\eta_\rho}(w; \mu)[h, h]}}, \quad \forall h \in \hat{\mathbb{E}} \times \mathbb{E}, h \neq 0. \quad (86)$$

Choosing

$$h = \left((D_{\hat{x}\hat{x}}^2 \eta_\rho)^{-1} \nabla_{\hat{x}} \eta_\rho, -(D_{ss}^2 \eta_\rho)^{-1} \nabla_s \eta_\rho \right),$$

inequality (86) holds with equality, which completes the proof. \square

The preceding estimates quantify the sensitivity of the reduced BAL function with respect to the smoothing parameter. The following lemma is the key step in the path-following analysis: it shows that, if the current point is in the neighborhood associated with μ , then the same point remains sufficiently close to the new central path after replacing μ by $\sigma\mu$.

Lemma 4 *Let $\rho > 0$, $\mu > 0$, $\kappa = 0.1$, and $\mu^+ = \sigma\mu$ with*

$$\sigma = 1 - \frac{\ln(\gamma)}{2\sqrt{\nu} + \ln(\gamma)}, \text{ where } \gamma := \frac{2\kappa + \sqrt{2}}{\kappa + \sqrt{2}}. \quad (87)$$

If $\xi_\rho(w; \mu) \leq \kappa$, then

$$\xi_\rho(w; \mu^+) \leq 2\kappa. \quad (88)$$

Proof For any nonzero $h \in \hat{\mathbb{E}} \times \mathbb{E}$, define the function $\psi : \mathbb{R}_{++} \times \hat{\mathbb{E}} \times \mathbb{E} \rightarrow \mathbb{R}$ as

$$\psi(\tau, h) := \frac{\langle \nabla_w \eta_\rho(w; \tau), h \rangle^2}{\tau S_{\eta_\rho}(w; \tau)[h, h]}.$$

Differentiating $\psi(\tau, h)$ with respect to τ gives

$$\begin{aligned} \psi'(\tau, h) &= \frac{2\langle \nabla_w \eta_\rho(w; \tau), h \rangle \cdot \langle \nabla_w \eta'_\rho(w; \tau), h \rangle}{\tau S_{\eta_\rho}(w; \tau)[h, h]} - \frac{\langle \nabla_w \eta_\rho(w; \tau), h \rangle^2}{\tau^2 S_{\eta_\rho}(w; \tau)[h, h]} \\ &\quad - \frac{\langle \nabla_w \eta_\rho(w; \tau), h \rangle^2 S'_{\eta_\rho}(w; \tau)[h, h]}{\tau (S_{\eta_\rho}(w; \tau)[h, h])^2}. \end{aligned}$$

Let $\tau \in [\mu^+, \mu]$. It follows from Theorems 9–10 that

$$\begin{aligned} |\psi'(\tau, h)| &\leq \sqrt{\frac{8\nu}{\tau^2}} \sqrt{\psi(\tau, h)} + \frac{2 + 2\sqrt{\nu}}{\tau} \psi(\tau, h) \\ &\leq \sqrt{\frac{8\nu}{(\mu^+)^2}} \sqrt{\psi(\tau, h)} + \frac{2 + 2\sqrt{\nu}}{\mu^+} \psi(\tau, h). \end{aligned}$$

Define $c_1 := \frac{1 + \sqrt{\nu}}{\mu^+}$ and $\Psi(\tau, h) := e^{c_1 \tau} \sqrt{\psi(\tau, h)}$. We have

$$-\Psi'(\tau, h) \leq e^{c_1 \tau} \frac{\sqrt{2\nu}}{\mu^+}. \quad (89)$$

Integrating both sides of (89) over $[\mu^+, \mu]$ yields

$$\Psi(\mu^+, h) - \Psi(\mu, h) \leq \frac{\sqrt{2\nu}}{\mu^+} \frac{1}{c_1} (e^{c_1 \mu} - e^{c_1 \mu^+}).$$

This implies that for any nonzero direction $h \in \hat{\mathbb{E}} \times \mathbb{E}$,

$$\begin{aligned} &\sqrt{\psi(\mu^+, h)} \\ &\leq e^{c_1(\mu - \mu^+)} \sqrt{\psi(\mu, h)} + \frac{\sqrt{2\nu}}{\mu^+} \frac{1}{c_1} (e^{c_1(\mu - \mu^+)} - 1) \\ &\leq e^{c_1(\mu - \mu^+)} \xi_\rho(w; \mu) + \frac{\sqrt{2\nu}}{\mu^+} \frac{1}{c_1} (e^{c_1(\mu - \mu^+)} - 1), \end{aligned} \quad (90)$$

where the last inequality follows from Lemma 3. Since (90) holds for every nonzero direction $h \in \hat{\mathbb{E}} \times \mathbb{E}$, we conclude by Lemma 3 again that

$$\xi_\rho(w; \mu^+) \leq e^{c_1(\mu - \mu^+)} \xi_\rho(w; \mu) + \frac{\sqrt{2\nu}}{\mu^+} \frac{1}{c_1} \left(e^{c_1(\mu - \mu^+)} - 1 \right). \quad (91)$$

Recall $\mu^+ = \sigma\mu$. Let

$$\begin{cases} \alpha_1(\sigma) := e^{c_1(\mu - \mu^+)} = e^{(1+\sqrt{\nu})(\frac{1}{\sigma} - 1)}, \\ \alpha_2 := \frac{\sqrt{2\nu}}{\mu^+} \frac{1}{c_1} = \frac{\sqrt{2\nu}}{1+\sqrt{\nu}}. \end{cases} \quad (92)$$

It can be verified that

$$\alpha_1(\sigma) = e^{(1+\sqrt{\nu}) \cdot \frac{\ln(\gamma)}{2\sqrt{\nu}}} \leq \gamma \quad \text{and} \quad \alpha_2 \leq \sqrt{2},$$

whenever $\sigma = 1 - \frac{\ln(\gamma)}{2\sqrt{\nu} + \ln(\gamma)}$.

Combining this estimate with (91) and (92), we get

$$\xi_\rho(w; \mu^+) \leq \alpha_1(\sigma)\kappa + \alpha_2(\alpha_1(\sigma) - 1) \leq 2\kappa,$$

which completes the proof. \square

Building on these estimates, we establish the main result of the paper: Algorithm 2 admits a polynomial iteration complexity of order $\mathcal{O}(\sqrt{\nu} \ln(1/\varepsilon))$, matching the best-known complexity of classical short-step IPMs.

Theorem 12 *Let $\rho > 0$, $\kappa = 0.1$, and choose σ as defined in (87). Suppose that the initial point $v^{(0)}$ is generated by Algorithm 1. Then Algorithm 2 requires at most $\mathcal{O}(\sqrt{\nu} \ln(\mu^{(0)}/\varepsilon))$ iterations to attain the desired accuracy ε .*

Proof We first show the iterates remain in the neighborhood $\mathcal{N}(\kappa, \mu^{(k)}, \rho)$ for any $k \geq 0$. The claim holds for $k = 0$ by the initialization. Suppose that $v^{(k)} \in \mathcal{N}(\kappa, \mu^{(k)}, \rho)$, which implies that

$$\xi_\rho(w^{(k)}; \mu^{(k)}) \leq \kappa.$$

If $\mu^{(k)} \leq \varepsilon$, the algorithm terminates. Otherwise, the smoothing parameter is reduced according to $\mu^{(k+1)} = \sigma\mu^{(k)}$. Applying Lemma 4 with $w = w^{(k)}$, $\mu = \mu^{(k)}$, $\mu^+ = \mu^{(k+1)}$, we obtain

$$\xi_\rho(w^{(k)}; \mu^{(k+1)}) \leq 2\kappa.$$

Since $\kappa = 0.1$, we have $2\kappa = 0.2 < 2 - \sqrt{3}$. Let $w^{(k+1)}$ denote the point obtained after one full Newton step. By Theorem 3(iii)

$$\xi_\rho(w^{(k+1)}; \mu^{(k+1)}) \leq \frac{\xi_\rho(w^{(k)}; \mu^{(k+1)})}{2} \leq \kappa.$$

This, combined with (65), implies that $v^{(k+1)} \in \mathcal{N}(\kappa, \mu^{(k+1)}, \rho)$. By induction, we conclude that $v^{(k)}$ remains in the neighborhood $\mathcal{N}(\kappa, \mu^{(k)}, \rho)$ for any $k \geq 0$.

Now we bound the number of Newton steps. Since $\mu^{(k)} = \sigma^k \mu^{(0)}$, the stopping criterion $\mu^{(k)} \leq \varepsilon$ of Algorithm 2 is satisfied whenever

$$k \geq \frac{\ln(\mu^{(0)}/\varepsilon)}{\ln(1/\sigma)}.$$

Consequently, Algorithm 2 requires at most

$$-\ln\left(\frac{\mu^{(0)}}{\varepsilon}\right) / \ln(\sigma) + 1 = \mathcal{O}\left(\sqrt{\nu} \ln\left(\frac{\mu^{(0)}}{\varepsilon}\right)\right)$$

iterations to obtain an approximate KKT triple. \square

Remark 5 Combining Theorems 8 and 12, we obtain that the first phase of PFSNM requires at most $\mathcal{O}\left(1 + \frac{4t^{(0)}}{\kappa} \Theta_1\left(\frac{\theta_\rho(w^{(0,0)}; \mu^{(0)})}{\mu^{(0)}}\right)\right)$ iterations, whereas the second phase of PFSNM admits an iteration complexity of $\mathcal{O}\left(\sqrt{\nu} \ln\left(\frac{\mu^{(0)}}{\varepsilon}\right)\right)$. Therefore, the overall iteration complexity is

$$\mathcal{O}\left(1 + \frac{4t^{(0)}}{\kappa} \Theta_1\left(\frac{\theta_\rho(w^{(0,0)}; \mu^{(0)})}{\mu^{(0)}}\right)\right) + \mathcal{O}\left(\sqrt{\nu} \ln\left(\frac{\mu^{(0)}}{\varepsilon}\right)\right).$$

Since the first term is independent of ε , the above bound can be written more compactly as $\mathcal{O}(\sqrt{\nu} \ln(1/\varepsilon))$.

6 Computational results

To validate the effectiveness of the proposed method (PFSNM), this section reports numerical results on three benchmarks and compares PFSNM with several widely used conic programming solvers, including SDPT3 [42], SeDuMi [40], ECOS [12], and Clarabel [16]. The test instances consist of linear programs from the NETLIB collection¹, convex quadratic programs (QP) from the Maros–Mészáros collection², and second-order cone programs arising from square-root Lasso formulations constructed using matrices from the SuiteSparse Matrix Collection³. All computational results are obtained on a Windows 10 personal computer equipped with an Intel i5-8300H processor (4 cores, 8 threads, 2.3 GHz) and 16 GB of RAM. The proposed method is implemented in C.

We evaluate solver performance using performance profiles [11] and the shifted geometric mean (SGM)⁴. Let \mathcal{P} denote the benchmark set and \mathcal{S} denote the set of solvers. For each problem $p \in \mathcal{P}$ and solver $s \in \mathcal{S}$, let $t_{p,s}$ be the runtime, and define the performance ratio

$$r_{p,s} = \frac{t_{p,s}}{\min_{s' \in \mathcal{S}} t_{p,s'}} \in [1, \infty],$$

¹ <https://netlib.org/lp/data/>

² <https://www.doc.ic.ac.uk/~im/>

³ <https://sparse.tamu.edu/>

⁴ <https://plato.asu.edu/ftp/shgeom.html>

where $r_{p,s} = \infty$ if solver s fails to solve problem p within the time limit of 1000 seconds. The performance profile is given by

$$\rho_s(\tau) = \frac{1}{|\mathcal{P}|} \left| \{p \in \mathcal{P} : r_{p,s} \leq \tau\} \right|, \quad \tau \geq 1,$$

which measures the fraction of instances for which s is within a factor τ of the best solver. The value at $\tau = 1$ reflects the frequency with which solver s is the fastest, while the limiting value as τ grows measures its empirical success rate. In addition, we summarize the overall performance via the shifted geometric mean (with offset = 1)

$$\text{SGM}_s = \exp \left(\sum_{p \in \mathcal{P}} \frac{1}{|\mathcal{P}|} \ln (\max\{1, t_{p,s} + \text{offset}\}) \right) - \text{offset},$$

so that smaller values indicate better aggregate efficiency while being relatively insensitive to a small number of difficult instances.

6.1 Linear programs

We first test the solvers on linear programs from the widely used NETLIB collection. The results are summarized in Table 2 and Fig. 3.

Table 2 reports the solved ratios together with the shifted geometric means. The main observation is that PFSNM achieves a favorable balance between robustness and efficiency on this benchmark. In particular, it achieves the best aggregate runtime behavior as measured by the SGM without compromising reliability, whereas competing solvers exhibit either a lower success rate or a noticeably larger SGM. This indicates that the advantage of PFSNM on NETLIB is consistent across instances, reflecting a favorable overall balance between convergence robustness and computational cost.

Table 2: Solved ratios and SGMs of PFSNM, SDPT3, SeDuMi, ECOS, and Clarabel on the NETLIB collection.

Solver	PFSNM	SDPT3	SeDuMi	ECOS	Clarabel
Solved ratio	100%	73.47%	93.88%	95.92%	97.96%
SGM	1.0000	25.0299	3.5985	2.7778	2.0520

Figure 3 provides a more intuitive perspective through performance profiles. The curve of PFSNM stays above the competing solvers over essentially the entire range of τ . This behavior indicates that PFSNM is frequently the fastest among the five solvers on a large fraction of the benchmark set. Furthermore, $\rho_s(\tau)$ for PFSNM approaches 1 as τ increases, which means that it successfully solves all LP instances under the imposed limits. In contrast, the profiles of the other solvers level off below 1, and their slower rise for small τ indicates weaker performance on instances with comparable runtimes.

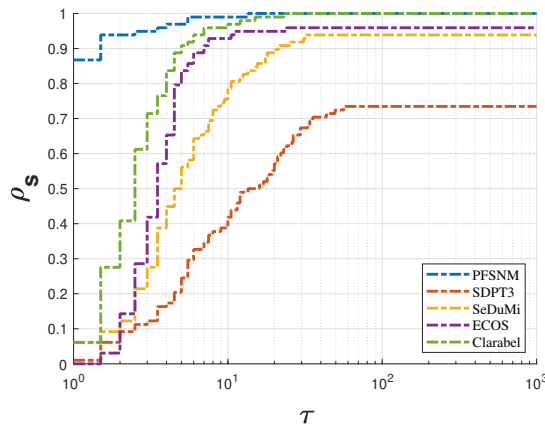


Fig. 3: Performance profiles of PFSNM, SDPT3, SeDuMi, ECOS, and Clarabel on the NETLIB collection

6.2 Quadratic programs

We next consider convex quadratic programs from the Maros–Mészáros collection, a standard benchmark for QP problems. The results are summarized in Table 3 and Fig. 4.

Table 3 suggests that PFSNM is competitive in terms of aggregate efficiency, although it is not the best-performing solver overall. In particular, its shifted geometric mean is the second-best among the tested solvers (about 2.66), whereas Clarabel attains the best value (normalized to 1.00). At the same time, the solved ratios indicate that Clarabel succeeds on a larger fraction of the QP instances (about 91.3%), while PFSNM solves a smaller but still substantial fraction (about 82.6%). Overall, the table indicates that the main difference between PFSNM and the best solver on this benchmark lies in robustness on a subset of instances.

Table 3: Solved ratios and SGMs of PFSNM, SDPT3, SeDuMi, ECOS, and Clarabel on the Maros–Mészáros collection.

Solver	PFSNM	SDPT3	SeDuMi	ECOS	Clarabel
Solved ratio	82.61%	77.54%	83.33%	72.46%	91.30%
SGM	2.6598	8.1669	5.8094	7.7222	1.0000

Figure 4 provides a consistent view. The performance profile of PFSNM rises quickly for small values of τ , which indicates that when PFSNM succeeds, its runtimes are often close to those of the best solver on those instances. However, the limiting value of its profile remains below that of the most reliable solver, reflecting the gap in solved ratios reported in Table 3. Overall, the QP results show that PFSNM can be fast on the instances it solves. Improving robustness on

the more difficult subset of Maros–Mészáros problems would further enhance its performance on this benchmark.

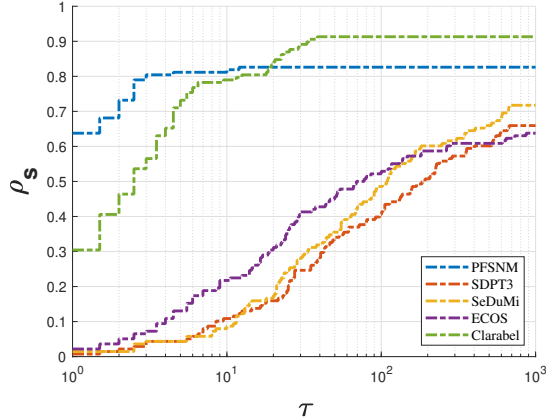


Fig. 4: Performance profiles of PFSNM, SDPT3, SeDuMi, ECOS, and Clarabel on the Maros–Mészáros collection

6.3 Second-order cone programs

Finally, we evaluate the solvers on a family of SOCP instances constructed from Lasso formulations. The data matrices are drawn from the SuiteSparse Matrix Collection, and each matrix is used to build a square-root Lasso problem [3, 24] of the form

$$\min_{y \in \mathbb{R}^n} \{ \|Dy - b\|_2 + \varrho \|y\|_1 \},$$

where $D \in \mathbb{R}^{d \times n}$ is a matrix from the SuiteSparse Matrix Collection, $b \in \mathbb{R}^d$ is a given vector, and ϱ is a penalty parameter. This problem is equivalent to the following SOCP reformulation:

$$\min \left\{ t + \varrho \sum_{i=1}^n (y_i^+ + y_i^-) \mid Dy^+ - Dy^- - r = b, (t, r) \in \mathbb{Q}^{d+1}, y^+, y^- \in \mathbb{R}_+^n \right\}.$$

Following [16], we choose $\varrho = \|D^\top b\|_\infty$. The vector b is set to the all-ones vector. The results are reported in Table 4 and Fig. 5.

Table 4 shows that all solvers solve all the instances, so the comparison is driven by efficiency rather than robustness. In this setting, PFSNM attains the smallest SGM (normalized to 1.0000). The closest competitor is Clarabel, with an SGM only slightly larger (about 1.0818), whereas the remaining solvers have clearly larger SGM values. Hence, the table indicates that PFSNM provides the best aggregate runtime performance on these Lasso-type SOCPs, with particularly close performance relative to Clarabel.

Table 4: Solved ratios and SGMs of PFSNM, SDPT3, SeDuMi, ECOS, and Clarabel on SOCP problems constructed from SuiteSparse matrices.

Solver	PFSNM	SDPT3	SeDuMi	ECOS	Clarabel
Solved ratio	100%	100%	100%	100%	100%
SGM	1.0000	3.5750	2.5645	2.3100	1.0818

Figure 5 is consistent with the table-based summary. Since all solvers succeed, the key difference lies in how quickly each profile rises near $\tau = 1$. The PFSNM curve increases the fastest and stays close to the best observed curve over a wide range of τ , meaning that it achieves the best or near-best runtime on a large fraction of instances. Combined with the SGM results, these experiments indicate that PFSNM offers strong and reliable performance on SOCP problems constructed from SuiteSparse matrices.

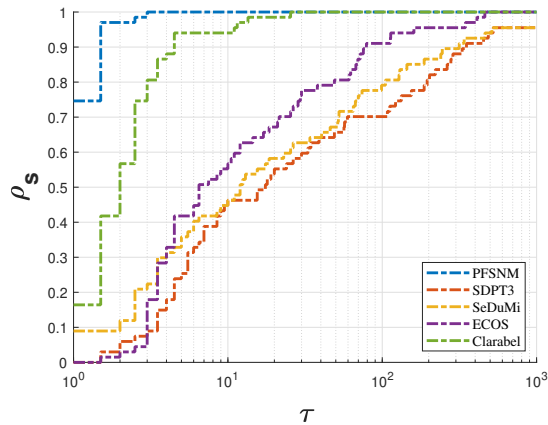


Fig. 5: Performance profiles of PFSNM, SDPT3, SeDuMi, ECOS, and Clarabel on SOCP problems constructed from SuiteSparse matrices

7 Conclusion

We have proposed a path-following smoothing Newton method for symmetric cone programming based on a reduced BAL function. The associated parameterized smooth system has been shown to be equivalent to the first-order optimality conditions of a structured minimax problem. This characterization makes it possible to analyze the proposed method within a self-concordant convex-concave framework. We have proved that the reduced BAL function is μ -self-concordant convex-concave and that the resulting method attains a worst-case iteration complexity of $O(\sqrt{\nu} \ln(1/\varepsilon))$. This iteration complexity matches the best-known short-step bound for IPMs on symmetric cones. Moreover, the reduced BAL function also yields Newton systems with an explicit Schur complement, which can be exploited

to reduce system-formation costs for important classes of symmetric cones. Numerical results indicate that the method is competitive on standard conic benchmarks.

A Auxiliary proofs

A.1 Proof of Proposition 1

Proof For any point $w = (\hat{x}, s) \in \hat{\mathbb{E}} \times \mathbb{E}$ and any direction $h_{\hat{x}} \in \hat{\mathbb{E}}$, define $h = (h_{\hat{x}}, 0) \in \hat{\mathbb{E}} \times \mathbb{E}$ and let $\varrho(t) = D^2 f(w + th)[h, h] = D_{\hat{x}\hat{x}}^2 f(w + th)[h_{\hat{x}}, h_{\hat{x}}]$. By the α -self-concordant convex-concave property of f , we have

$$\begin{aligned} \varrho'(t) &= D_{\hat{x}\hat{x}\hat{x}}^3 f(w + th)[h_{\hat{x}}, h_{\hat{x}}, h_{\hat{x}}] \\ &= D^3 f(w + th)[h, h, h] \\ &\leq \frac{2}{\alpha^{1/2}} (S_f(w + th)[h, h])^{3/2} \\ &= \frac{2}{\alpha^{1/2}} (D_{\hat{x}\hat{x}}^2 f(w + th)[h_{\hat{x}}, h_{\hat{x}}])^{3/2}. \end{aligned}$$

Taking $t = 0$ yields

$$|D_{\hat{x}\hat{x}\hat{x}}^3 f(w)[h_{\hat{x}}, h_{\hat{x}}, h_{\hat{x}}]| \leq \frac{2}{\alpha^{1/2}} (D_{\hat{x}\hat{x}}^2 f(w)[h_{\hat{x}}, h_{\hat{x}}])^{3/2}.$$

Moreover, for any $w \in \hat{\mathbb{E}} \times \mathbb{E}$ and any nonzero direction $h_{\hat{x}} \in \hat{\mathbb{E}}$,

$$D_{\hat{x}\hat{x}}^2 f(w)[h_{\hat{x}}, h_{\hat{x}}] > 0.$$

This implies that $f(\cdot, s)$ is nondegenerate α -self-concordant on $\hat{\mathbb{E}}$ for every $s \in \mathbb{E}$. An analogous argument shows that $-f(\hat{x}, \cdot)$ is nondegenerate α -self-concordant on \mathbb{E} for every $\hat{x} \in \hat{\mathbb{E}}$.

The conclusion in (ii) follows directly from [33, Proposition 9.1.1]. \square

A.2 Proof of Theorem 3(iv)

Proof Define

$$\begin{aligned} \xi_{\hat{x}}(w) &:= \left(\frac{1}{\alpha} \langle \nabla_{\hat{x}} f(w), (D_{\hat{x}\hat{x}}^2 f(w))^{-1} \nabla_{\hat{x}} f(w) \rangle \right)^{1/2}, \\ \xi_s(w) &:= \left(\frac{1}{\alpha} \langle \nabla_s f(w), (-D_{ss}^2 f(w))^{-1} \nabla_s f(w) \rangle \right)^{1/2}. \end{aligned}$$

By definition, $\xi(w)^2 = \xi_{\hat{x}}(w)^2 + \xi_s(w)^2$. Let $\varrho_s(\tilde{x}) = f(\tilde{x}, s)$ and $\hat{x}(s) = \arg \min_{\tilde{x}} \varrho_s(\tilde{x})$. Define $d := \hat{x} - \hat{x}(s)$. Recall that

$$\tilde{\delta}_{\hat{x}}(w) = \left(\frac{1}{\alpha} (d, D_{\hat{x}\hat{x}}^2 f(w) d) \right)^{1/2}.$$

By Proposition 1, $\varrho_s(\cdot)$ is α -self-concordant convex on $\hat{\mathbb{E}}$. Consequently, it follows from [33, Eq. (2.2.31)] that

$$\tilde{\delta}_{\hat{x}}(w) \leq 1 - (1 - 3\xi_{\hat{x}}(w))^{1/3} \leq 1 - (1 - 3\xi(w))^{1/3}.$$

Similarly, one has

$$\tilde{\delta}_s(w) \leq 1 - (1 - 3\xi_s(w))^{1/3} \leq 1 - (1 - 3\xi(w))^{1/3}.$$

Consequently

$$\max\{\tilde{\delta}_{\hat{x}}(w), \tilde{\delta}_s(w)\} \leq 1 - (1 - 3\xi(w))^{1/3}.$$

Furthermore, if $\xi(w) \leq 0.1$, then

$$\max\{\tilde{\delta}_{\hat{x}}(w), \tilde{\delta}_s(w)\} \leq 1 - 0.7^{1/3} < 0.2,$$

which completes the proof. \square

References

1. Alizadeh, F., Goldfarb, D.: Second-order cone programming. *Math. Program.* **95**(1), 3–51 (2003)
2. Beck, A.: *First-order methods in optimization*. SIAM, Philadelphia (2017)
3. Belloni, A., Chernozhukov, V., Wang, L.: Square-root lasso: pivotal recovery of sparse signals via conic programming. *Biometrika* **98**(4), 791–806 (2011)
4. Burke, J., Xu, S.: A non-interior predictor-corrector path following algorithm for the monotone linear complementarity problem. *Math. Program.* **87**(1), 113–130 (2000)
5. Burke, J.V., Xu, S.: The global linear convergence of a noninterior path-following algorithm for linear complementarity problems. *Math. Oper. Res.* **23**(3), 719–734 (1998)
6. Chan, Z.X., Sun, D.F.: Constraint nondegeneracy, strong regularity, and nonsingularity in semidefinite programming. *SIAM J. Optim.* **19**(1), 370–396 (2008)
7. Chen, B., Harker, P.T.: A non-interior-point continuation method for linear complementarity problems. *SIAM J. Matrix Anal. Appl.* **14**(4), 1168–1190 (1993)
8. Chen, X., Tseng, P.: Non-interior continuation methods for solving semidefinite complementarity problems. *Math. Program.* **95**(3), 431–474 (2003)
9. De Klerk, E.: *Aspects of semidefinite programming: interior point algorithms and selected applications*. Kluwer Academic Publishers, Dordrecht (2002)
10. De Klerk, E., Vallentin, F.: On the Turing model complexity of interior point methods for semidefinite programming. *SIAM J. Optim.* **26**(3), 1944–1961 (2016)
11. Dolan, E.D., Moré, J.J.: Benchmarking optimization software with performance profiles. *Math. Program.* **91**(2), 201–213 (2002)
12. Domahidi, A., Chu, E., Boyd, S.: ECOS: An SOCP solver for embedded systems. In: 2013 European Control Conference (ECC), pp. 3071–3076. IEEE (2013)
13. Engelke, S., Kanzow, C.: Predictor-corrector smoothing methods for linear programs with a more flexible update of the smoothing parameter. *Comput. Optim. Appl.* **23**(3), 299–320 (2002)
14. Faraut, J., Korányi, A.: *Analysis on symmetric cones*. Oxford University Press, New York (1994)
15. Fukushima, M., Luo, Z.Q., Tseng, P.: Smoothing functions for second-order-cone complementarity problems. *SIAM J. Optim.* **12**(2), 436–460 (2002)
16. Goulart, P.J., Chen, Y.: Clarabel: An interior-point solver for conic programs with quadratic objectives (2024). DOI 10.48550/arXiv.2405.12762
17. Hauser, R.A., Güler, O.: Self-scaled barrier functions on symmetric cones and their classification. *Found. Comput. Math.* **2**(2), 121–143 (2002)
18. Hotta, K., Inaba, M., Yoshise, A.: A complexity analysis of a smoothing method using CHKS-functions for monotone linear complementarity problems. *Comput. Optim. Appl.* **17**(2), 183–201 (2000)
19. Huang, Z.H., Qi, L.Q., Sun, D.F.: Sub-quadratic convergence of a smoothing Newton algorithm for the P_0 - and monotone LCP. *Math. Program.* **99**(3), 423–441 (2004)
20. Kanzow, C.: Some non-interior continuation methods for linear complementarity problems. *SIAM J. Matrix Anal. Appl.* **17**(4), 851–868 (1996)
21. Kanzow, C., Nagel, C.: Semidefinite programs: new search directions, smoothing-type methods, and numerical results. *SIAM J. Optim.* **13**(1), 1–23 (2002)
22. Kanzow, C., Pieper, H.: Jacobian smoothing methods for nonlinear complementarity problems. *SIAM J. Optim.* **9**(2), 342–373 (1999)
23. Kong, L.C., Sun, J., Xiu, N.H.: A regularized smoothing Newton method for symmetric cone complementarity problems. *SIAM J. Optim.* **19**(3), 1028–1047 (2008)
24. Liang, L., Sun, D.F., Toh, K.C.: An inexact augmented Lagrangian method for second-order cone programming with applications. *SIAM J. Optim.* **31**(3), 1748–1773 (2021)
25. Liang, L., Sun, D.F., Toh, K.C.: A squared smoothing Newton method for semidefinite programming. *Math. Oper. Res.* **50**(4), 2873–2908 (2024)
26. Liu, X.W., Dai, Y.H.: A globally convergent primal-dual interior-point relaxation method for nonlinear programs. *Math. Comp.* **89**(323), 1301–1329 (2020)
27. Liu, X.W., Dai, Y.H., Huang, Y.K.: A primal-dual interior-point relaxation method with global and rapidly local convergence for nonlinear programs. *Math. Methods Oper. Res.* **96**(3), 351–382 (2022)
28. Liu, X.W., Dai, Y.H., Huang, Y.K., Sun, J.: A novel augmented Lagrangian method of multipliers for optimization with general inequality constraints. *Math. Comp.* **92**(341), 1301–1330 (2023)

29. Liu, Y.J., Zhang, L.W., Wang, Y.H.: Analysis of a smoothing method for symmetric conic linear programming. *J. Appl. Math. Comput.* **22**(1), 133–148 (2006)
30. Monteiro, R.D., Zhang, Y.: A unified analysis for a class of long-step primal-dual path-following interior-point algorithms for semidefinite programming. *Math. Program.* **81**(3), 281–299 (1998)
31. Nemirovski, A.: On self-concordant convex–concave functions. *Optim. Methods Softw.* **11**(1–4), 303–384 (1999)
32. Nesterov, Y.: Long-step strategies in interior-point primal-dual methods. *Math. Program.* **76**(1), 47–94 (1997)
33. Nesterov, Y., Nemirovskii, A.: Interior-point polynomial algorithms in convex programming. SIAM, Philadelphia (1994)
34. Nesterov, Y.E., Todd, M.J.: Primal-dual interior-point methods for self-scaled cones. *SIAM J. Optim.* **8**(2), 324–364 (1998)
35. Nocedal, J., Wright, S.J.: Numerical optimization. Springer, New York (2006)
36. Peng, J.M., Lin, Z.H.: A non-interior continuation method for generalized linear complementarity problems. *Math. Program.* **86**(3), 533–563 (1999)
37. Qi, L.Q., Sun, D.F., Zhou, G.L.: A new look at smoothing Newton methods for nonlinear complementarity problems and box constrained variational inequalities. *Math. Program.* **87**(1), 1–35 (2000)
38. Schmieta, S.H., Alizadeh, F.: Extension of primal-dual interior point algorithms to symmetric cones. *Math. Program.* **96**(3), 409–438 (2003)
39. Smale, S.: Algorithms for solving equations. In: F. Cucker, R.S.C. Wong (eds.) *The Collected Papers of Stephen Smale*, vol. 3, pp. 1263–1286. World Scientific, Singapore (2000)
40. Sturm, J.F.: Using SeDuMi 1.02, a MATLAB toolbox for optimization over symmetric cones. *Optim. Methods Softw.* **11**(1–4), 625–653 (1999)
41. Sun, J., Sun, D.F., Qi, L.Q.: A squared smoothing Newton method for nonsmooth matrix equations and its applications in semidefinite optimization problems. *SIAM J. Optim.* **14**(3), 783–806 (2004)
42. Tütüncü, R.H., Toh, K.C., Todd, M.J.: Solving semidefinite-quadratic-linear programs using SDPT3. *Math. Program.* **95**(2), 189–217 (2003)
43. Vavasis, S.A., Ye, Y.Y.: A primal-dual interior point method whose running time depends only on the constraint matrix. *Math. Program.* **74**(1), 79–120 (1996)
44. Vieira, M.V.C.: Jordan algebraic approach to symmetric optimization. Ph.D. thesis, Delft University of Technology, Delft, The Netherlands (2007)
45. Wright, S.J.: Primal-dual interior-point methods. SIAM, Philadelphia (1997)
46. Xu, S., Burke, J.V.: A polynomial time interior-point path-following algorithm for LCP based on Chen-Harker-Kanzow smoothing techniques. *Math. Program.* **86**(1), 91–103 (1999)
47. Zhang, R.J., Liu, X.W., Dai, Y.H.: IPRQP: a primal-dual interior-point relaxation algorithm for convex quadratic programming. *J. Global Optim.* **87**(2–4), 1027–1053 (2023)
48. Zhang, R.J., Liu, X.W., Dai, Y.H.: IPRSDP: a primal-dual interior-point relaxation algorithm for semidefinite programming. *Comput. Optim. Appl.* **88**(1), 1–36 (2024)
49. Zhang, R.J., Wang, Z.W., Liu, X.W., Dai, Y.H.: IPRSOCP: a primal-dual interior-point relaxation algorithm for second-order cone programming. *J. Oper. Res. Soc. China* **14**(1), 1–31 (2026)
50. Zhao, Y.B., Li, D.: A globally and locally superlinearly convergent non-interior-point algorithm for P_0 LCPs. *SIAM J. Optim.* **13**(4), 1195–1221 (2003)